Quintessence Models with Tracking Behaviour

Jasmin Pielorz

Diplomarbeit in Physik
angefertigt im
Physikalischen Institut

vorgelegt der
Mathematisch-Naturwissenschaftlichen Fakultät
der
Rheinischen Friedrich-Wilhelms-Universität
Bonn

im Dezember 2002
(korrigierte Fassung März 2003)

Ich versichere, dass ich diese Arbeit selbständig verfasst und keine anderen als die angegebenen Quellen und Hilfsmittel benutzt sowie die Zitate kenntlich gemacht habe.

Referent:	Prof. Dr. Hans-Peter Nilles
Korreferent:	Prof. Dr. Ulf Danielsson

Danksagung

Zuerst möchte ich mich bei Prof. Dr. Hans-Peter Nilles bedanken. Er hat es mir ermöglicht, in seiner Gruppe an einem interessanten und aktuellen Thema der Kosmologie zu arbeiten.
Desweiteren bedanke ich mich bei allen Mitgliedern meiner Arbeitsgruppe für die angenehme Atmosphäre, namentlich bei Kang-Sin Choi, Ki-Young Choi, Dr. Athanasios Dedes, Priv. Doz. Dr. Stefan Förste, Florian Gmeiner, Dr. Gabriele Honecker, Mark Hillenbach, Prof. Dr. Jihn E. Kim, Dr. Hyun Min Lee, Prof. Dr. Marek Olechowski, Dr. Antonios Papazoglou, Dr. Marco Peloso, Dr. Ralph Schreyer, Dr. Pietro Slavich, Dr. Gianmassimo Tasinato, Martin Walter, Akın Wingerter und Dr. Max Zucker.
Außerdem danke ich Prof. Dr. Ulf Danielsson von der Universität Uppsala, der die Themenstellung angeregt hat, und sich bereiterklärt hat, die Kokorrektur dieser Arbeit zu übernehmen.
Für die besondere Zusammenarbeit und fachliche Unterstützung im letzten Jahr danke ich Marco Peloso. Auch für die Unterstützung durch Akın Wingerter, Gianmassimo Tasinato und Andreas Wißkirchen, insbesondere in den letzten Wochen, möchte ich mich bei diesen sehr bedanken.
Ich bedanke mich bei Martin Kilbinger und Renate Lampert für das Korrekturlesen und bei allen meinen Freunden und meiner Familie, die mich nur in den richtigen Momenten vom Arbeiten abgehalten haben. Ganz besonders bedanken möchte ich mich bei meinem Freund Christoph Lampert, ohne dessen Unterstützung ich die Diplomarbeitszeit wohl kaum überstanden hätte. Schließlich danke ich der Carl-Duisberg-Stiftung für ihre finanzielle Unterstützung meines Studiums.

Contents

Chapter 1

Introduction

Classical view of the universe

From observations we know that our universe is homogeneous and isotropic on large scales, i.e. matter and radiation are evenly distributed and without any privileged direction. This is often referred to as the *Cosmological Principle*. Additionally, we can infer from the cosmic redshift that our universe is expanding. The light element abundance indicates that this has been the case since an early era in which the universe was hot and dense. This idea of a universe which evolved from an initial singularity is called the *Hot Big Bang model*. The Cosmic Microwave Background (CMB) which is observed at present times is interpreted as the relic radiation which is caused by the cooling of the expanding universe [1].

Following Newton's law of gravity it was widely accepted that the gravitational attraction among the constituents of the universe (radiation and matter) causes the expansion to be decelerated until present times.

However, during recent years, several observational data contradicted this picture. Investigations of the cluster abundance state that only one third of the universe consists of matter [2, 3]. In addition, we learn from Cosmic Microwave Background observations [4] that our universe is close to flat. So the missing contribution has to be a form of energy which does not cluster, otherwise we would have observed it, e.g. in the rotational curves of galaxies. Even more surprising were the recent results from the observation of distant supernovae. Against the prevailing opinion the data clearly favour a universe which undergoes a phase of *recent acceleration* [5, 6]. Combining the results with the data obtained from CMB and cluster measurements (see figure 1.1) one sees the necessity of a form of *dark energy* which repulses the gravitational attraction. Using general relativity, it is possible to have an accelerating universe by introducing a non-zero, positive cosmological constant.

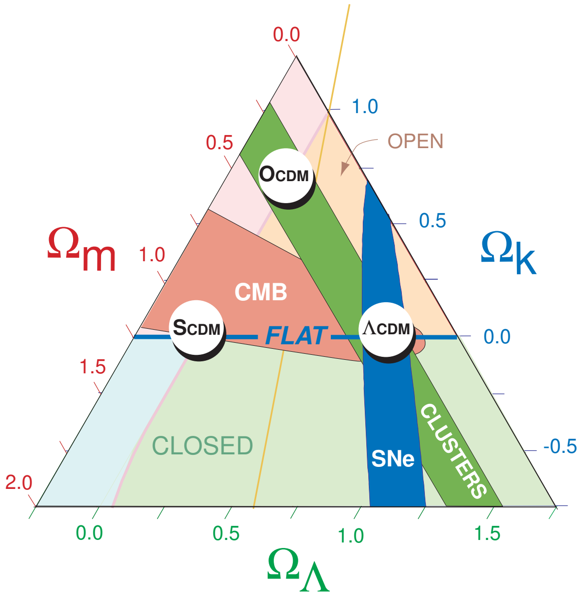

Figure 1.1: Cosmic triangle with constraints from different observations [7]. The data clearly favour the cosmological constant model (ΛCDM) over a pure matter universe (SCDM) or a universe with dominant curvature (OCDM).

The idea of supernovae Type Ia observations

One method to determine the expansion rate of the universe is based on measuring the *observed brightness* and the *redshift* of astronomical objects. From the redshift of an object we can deduce the point of time when its light was emitted. The relation between the two quantities depends on the underlying model. The difficulty lies in associating a physical distance with this point of time. For this reason cosmologists introduced the *luminosity distance*

$$d_L^2 = \frac{\mathcal{L}}{4\pi\mathcal{F}} \tag{1.1}$$

which decribes the fact that the intensity of a light signal decreases with the inverse-square of the distance [1]. Measuring the incoming flux $\mathcal{F}$ of an object with known absolute luminosity $\mathcal{L}$ it is possible to infer the corresponding luminosity distance.

Suitable objects for this purpose are supernovae of Type Ia. They have characteristic light curves which are well known from samples in our galactic neighbourhood. The absolute luminosity $\mathcal{L}$ for more distant supernovae can be deduced from these samples. Because of this property and their strong brightness even at high redshifts, Type Ia supernovae are often referred to

as *standard candles* [7]. At the moment two research groups investigate supernovae at high redshifts: The Supernova Cosmology Project [5] and the High-Z Supernova Search [8, 9]. Both agree that the observed brightness is fainter than expected which they explain by accelerated expansion.
In order to explain the larger luminosity distance at a fixed redshift one assumes the presence of a cosmological constant or more general of a *dark energy* that causes the acceleration. These conclusions have to be taken with caution, since we cannot exclude that evolutionary effects modify the absolute luminosity of the supernovae. Alternative ideas to explain the decrease of the observed luminosity have been proposed (e.g. intergalactic dust, mixing of photons with axions [10]). In spite of these aspects, the interpretation that the universe is accelerating is favoured, since it is in agreement with observations from the CMB anisotropies and clusters.

Problems with a cosmological constant

For the present phase of accelerated expansion we need a form of energy that "counteracts gravity". General relativity allows the presence of such an energy with a sufficiently negative pressure. The simplest form for this energy is provided by a cosmological constant term that can be added to Einstein's equations. In this case it is important to notice that the effective energy of the ground state really is of importance. This is due to the fact that gravity couples directly to the vacuum energy. In most other physical contexts, we are mainly interested in the potential differences as e.g. in case of a falling object which loses potential energy.
A cosmological constant model is consistent with observations of the CMB and the clusters (see figure 1.1). Thus, it would seem natural to accept the presence of a cosmological constant. On the other hand, a contribution from the vacuum to the content of the universe has to be explained judiciously from the theoretical point of view. There is even more a need for a good explanation since the measured value of Ω_Λ^0 and the Hubble constant H_0 fix a possible vacuum energy contribution to

$$\rho_{vacuum} \approx 10^{-120} M_P^4 = (3 \cdot 10^{-3}\,\mathrm{eV})^4 \;. \tag{1.2}$$

While, at the classical level, one can arbitrarily choose the value of the vacuum energy, one must remember that this value will receive new contributions considering quantum effects. The question is why all these contributions – which are in the order of typical fundamental scales in particle physics – should add up to this small value. If for example supersymmetry (SUSY) is broken at the TeV scale, one would expect $\rho_{vac} \sim (1\mathrm{TeV})^4$. Because of

this big gap between the scales, a fine-tuning of the parameters is required to explain the non-zero vacuum expectation value (vev). This is known as the *cosmological constant problem* [11, 12].
A second problem associated with a cosmological constant is the so-called *coincidence problem.* The question is why matter and vacuum energy density are of the same order today. While the vacuum energy stays constant the other contributions decrease rapidly during the whole evolution of the universe. Therefore, their initial values have to be extraordinarily fine-tuned in order to have the energy densities at the same order today. Moreover, the fine-tuning required increases if the initial redshift of the universe increases. We will later refer to this problem as the *fine-tuning problem of the initial values.*

Quintessence as a candidate for a dark energy

The simplest approach to solve the above problems is to impose the vacuum energy to be *exactly zero.* Usually this is done by using a symmetry argument. One example would be unbroken supersymmetry. However, since SUSY is broken, it can of course not help us in this specific case. We can be less demanding, simply *assuming* $\rho_{vac} = 0$ and then explaining the observed acceleration by some other form of dark energy. One possibility is to consider the dynamics of a sufficiently slowly rolling scalar field which mimics the behaviour of a cosmological constant at the present time. This type of model is often referred to as *quintessence* [13, 14, 15, 16]. Such fields are motivated theoretically in models where supersymmetry is dynamically broken by gaugino condensation [17]. Since the vev of the condensate depends on the value of the dilaton field, it could mimic a quintessential potential [11].
In this thesis, we will discuss in particular *quintessence models with tracker fields* [16, 18, 19]. These models are characterized by the existence of an attractor[1]. After the scaling of a free parameter in the potential, we can use this property to address the coincidence problem mentioned above. Since only one cosmological track is then possible, tracking quintessence models achieve insensitivity to initial conditions. A detailed analysis of this concept is the main topic of this thesis.
To emphasize how an overall insensitivity is obtained, we will additionaly consider the example of a scalar field model without this property [20, 21]. Although the field is chosen to mimic matter, it can produce a finite phase of acceleration which depends on the initial values. This results in much more

[1] As an attractor we denote a dedicated element in the space of solutions to the scalar field's equation of motion to which all other solutions are drawn (see chapter 4).

constraints on the range of the initial conditions than in the case of standard quintessence models with tracking behaviour. The details of the construction are given in chapter 5.

Observational constraints for quintessence

In physics, it is important to have a "predictive" theory which can be the subject to observational tests. In most cases the behaviour of quintessence differs from that of a cosmological constant. The acceleration changes during the evolution and the equation of state can vary. Since supernova Type Ia measurements are sensitive to the stage where the dark energy is dominant, we have a realistic chance to "test" quintessence [6]. For this reason, one chapter of the thesis discusses in how far quintessential models can be distinguished from a cosmological constant model by supernovae Type Ia measurements. More statistical studies of supernovae at higher z could give further insight into the nature of the dark energy.

Overview of the thesis

The thesis is structured as follows: we start in chapter 2 with a summary of the most important definitions and equations of the standard model of cosmology.
In chapter 3, we discuss the restrictions from supernova Type Ia measurements on the equation of state of the dark energy and the redshift at which the predicted acceleration begins.
Chapter 4 gives a description of standard quintessence models with tracking behaviour. It starts with the notion of tracker fields in section 4.1 and 4.2, where we can give a criterion to determine the tracker behaviour of a given potential. In section 4.3 the characteristic evolution of the quintessence energy density is discussed. We proceed in section 4.4 with the formulation of four constraints a tracker potential has to fulfill in order to end up with a reasonable model. Afterwards, we test these constraints on three single field quintessence potentials. Finally, in the last section of this chapter, the fine-tuning of initial values for an arbitrary tracker potential is investigated.
In chapter 5, we consider the exponential potential as an alternative quintessence model which leads to a finite acceleration phase of the universe. After a brief discussion of the tracker properties in section 5.1, we study the evolution of the energy density starting from the slow roll regime in the situation of the exponential potential in section 5.2. Moreover, we explain in detail how a limited stage of accelerated expansion can be achieved although the

tracker solution of the exponential potential behaves like an effective matter component. Section 5.3 closes this chapter with a reconsideration of the fine-tuning problem of the initial values in case of the exponential potential. Finally, chapter 6 gives the conclusions of this thesis.
In appendix A, we give a detailed derivation for the tracker criterion, whereas in appendix B, we deduce the approximation for the value where Q freezes in full length. Additionally, in appendix C, we present the differential equations used for the numerical simulations of the quintessence evolution.

Chapter 2

The standard model of cosmology

The considerations in this thesis are based on the *standard model of cosmology* [1, 22]. Therefore this chapter summarizes the most important definitions and equations of the Big Bang cosmology which we will need in the following.
The metric for a homogeneous and isotropic universe is the *Friedmann-Robertson-Walker* (FRW) metric with the line element

$$ds^2 = dt^2 - a^2 \{\frac{dr^2}{1 - kr^2} + r^2 d\theta^2 + r^2 \sin^2\theta d\varphi^2\} \tag{2.1}$$

where (r, θ, φ) are spherical coordinates, $a = a(t)$ denotes the scale factor and k is the curvature. The *scale factor* is a relative length which varies according to the expansion or contraction of the universe, whereas the *curvature* determines the underlying geometry of the universe. Through rescaling of a and r one can always set k equal to 0 or ± 1. For $k = 0$, one has a flat, euclidian space; for $k = -1$ a hyperbolic, open space; finally, $k = 1$ corresponds to an elliptical, closed space.
The expansion of the universe causes a *cosmic redshift* z in the wavelength of photons that are emitted at a time t_1 and detected at the present time t_0. It is defined by the ratio of detected to emitted wavelength:

$$1 + z \equiv \frac{\lambda(t_0)}{\lambda(t_1)} = \frac{a(t_0)}{a(t_1)} \ . \tag{2.2}$$

It is common to introduce a timescale based on z, where $z = 0$ denotes the present time and higher values of z correspond to earlier times.
The contents of the universe is customarily assumed to have the form of a perfect fluid. For a homogeneous distribution of the energy density $\rho = \rho(t)$

and the pressure $p = p(t)$, one recovers from Einstein's field equations and the FRW metric (2.1) the *Friedmann equations*:

$$H^2 \equiv \left(\frac{\dot{a}}{a}\right)^2 = \frac{8\pi G}{3}\rho - \frac{k}{a^2}\,, \tag{2.3}$$

$$\frac{\ddot{a}}{a} = -\frac{4\pi G}{3}\left(\rho + 3p\right) \tag{2.4}$$

where H is the *Hubble parameter*, the dots denote derivatives with respect to t, $G = 1/M_p^2$ and $M_p \simeq 1.22 \cdot 10^{19}$ GeV is the Planck mass. In general, the energy density ρ contains contributions from different species, e.g. from matter, radiation or a vacuum energy density. A contribution from the vacuum enters in the energy density as a cosmological constant term

$$\rho_\Lambda \equiv \frac{\Lambda}{8\pi G}\,. \tag{2.5}$$

It is common to give the different contributions to the contents of the universe in relative energy densities. For this reason one defines the *critical density*[1]

$$\rho_{crit} \equiv \frac{3H^2}{8\pi G}\,. \tag{2.6}$$

This equation corresponds to the Friedmann equation (2.3) for a flat universe (i.e. $k = 0$). The relative contribution of a single species to the total energy density ρ_{crit} is customarily given in terms of the ratio

$$\Omega_i \equiv \frac{\rho_i}{\rho_{crit}}\,. \tag{2.7}$$

The sum of all species in the universe defines the total energy density parameter Ω. Introducing this quantity allows to rewrite the Friedmann equation (2.3) as:

$$\frac{k}{H^2 a^2} = \Omega - 1\,. \tag{2.8}$$

If one now defines

$$\Omega_k \equiv -\frac{k}{a^2 H^2} \tag{2.9}$$

[1]Note that ρ_{crit} varies with time according to the Hubble parameter.

for the curvature, we have

$$\Omega_k + \Omega = 1 \ . \tag{2.10}$$

For a flat universe the Friedmann equations (2.3) and (2.4) can easily be solved. For this it is useful to characterize different species by their equations of state

$$w_i \equiv \frac{p_i(t)}{\rho_i(t)} \tag{2.11}$$

where w_i is independent of time for the most common species (see table 2.1). Combining the Friedmann equations (2.3) and (2.4) for a flat universe with the previous definition (2.11) yields

$$\dot{\rho} = -3H\,(1+w)\,\rho \ . \tag{2.12}$$

To guarantee the uniqueness of the solution one assumes the universe to have a single dominant species (i.e. $\rho_i \simeq \rho$).[2] Then equation (2.12) is solved by

$$\rho \propto a^{-3(1+w)} \ . \tag{2.13}$$

Accordingly, we find for the scale factor the following solutions:

$$a \propto t^{\frac{2}{3(1+w)}} \qquad \text{for}\, w \neq -1 \ , \tag{2.14}$$

$$a \propto e^{Ht} \qquad \text{for}\, w = -1 \ . \tag{2.15}$$

For the most standard species we have summarized the results in table (2.1).

	w	p	ρ	a
Radiation	$\frac{1}{3}$	$\frac{\rho}{3}$	$\propto a^{-4}$	$\propto t^{\frac{1}{2}}$
Matter	0	0	$\propto a^{-3}$	$\propto t^{\frac{2}{3}}$
Vacuum Energy	-1	$-\rho$	$\propto const$	$\propto e^{Ht}$

Table 2.1: Equation of state and scale factor for the most standard components

From figure 2.1 we see that the energy density of matter decreases more slowly than the one of radiation as the universe expands. This leads us to conclude that the radiation was dominant in the past and has been overtaken by the matter energy density at a certain point of time which we denote by

[2] This can be done with good accuracy during most of the evolution of the universe (see figure 2.1)

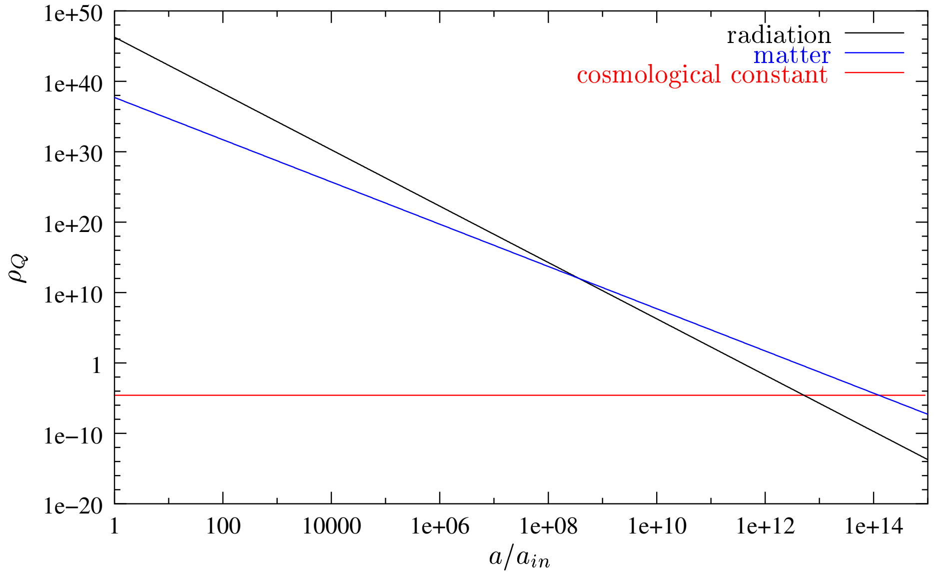

Figure 2.1: Schematic plot of the energy density versus the scale factor for the species given in table 2.1.

matter-radiation equality z_{eq}. For the same reason a cosmological constant will finally dominate over matter and radiation as the universe expands. Among these three species, only the vacuum energy density can be responsible for an accelerating universe. In general, combining equations (2.4) and (2.11) yields

$$\frac{\ddot{a}}{a} = -\frac{4\pi G}{3}(1 + 3w)\,\rho \tag{2.16}$$

and only if there is a dominant component with an equation of state $w < -\frac{1}{3}$, $\ddot{a}$ becomes positive and the universe accelerates.

Chapter 3

Present acceleration of a universe with dark energy and cold dark matter

Astronomical measurements of the cosmic microwave background, cluster abundance and supernovae Type Ia favour a flat universe with $\Omega_m \simeq 1/3$ and increasing expansion rate [7]. Since also the contribution of matter to the total density parameter is smaller than 1, a so-called *dark energy* component has to be introduced in order to be consistent with a flat universe. To cause accelerated expansion, a negative pressure is required for the dark energy. In this chapter we examine the nature of a possible dark energy contribution, by trying to restrict the range of its equation of state w_X. Since the observations of supernova Type Ia are sensitive to the expansion rate of the universe and thus to w_X, we can compare them with our theoretical results.
In section 3.1 we derive an expression for the luminosity distance of a supernova in terms of its redshift and w_X. The comparison with supernova data confirms the existence of a dark energy component but does not allow to distinguish between the various models. Section 3.2 deals with the discussion at which redshift z_{acc} the universe started its present accelerated phase. Indeed, the energy density of the species X decreases more slowly than the one of matter while the universe is expanding, so that at early times ($z > z_{acc}$) matter was dominant and the universe in a stage of decelerated expansion. In a w_X-Ω_m^0 plane the theoretical curves for different values of z_{acc} are compared with confidence contour plots obtained from supernova measurements. Again, no definite conclusions on w_X are possible. But if we require $\Omega_m^0 \approx 1/3$ the range of w_X can be restricted to $w_X \lesssim -0.6$. This leaves the possibility of considering alternative models apart from a pure cosmological constant model.

3.1 Determination of w_X from supernova Type Ia data

Our aim is to examine whether the current acceleration of the universe is caused by other forms of *dark energy* ρ_X rather than a pure cosmological constant.[1] For this reason we compare theoretical curves of the luminosity distance d_L with data obtained from supernova Type Ia measurements [7, 5, 6]. For our analysis we consider a flat universe ($k = 0$) well after matter-radiation equality. That is, we take into account the presence of matter and a form of *dark energy* with a variable equation of state $w_X = w_X(z)$. To decide which model fits the observation best, we express the luminosity distance d_L of a supernova in terms of its redshift and the equation of state w_X. The luminosity distance itself is inferred from the incoming flux on the earth of the observed supernovae. Since in the end the equation of state w_X remains as the only unknown quanitity, the procedure outlined allows to estimate its value.

3.1.1 Theoretical predictions

We start by introducing the deceleration parameter

$$q(z) \equiv \left(-\frac{\ddot{a}}{a}\right)/H^2(z) = \frac{\mathrm{d}H^{-1}(z)}{\mathrm{d}t} - 1 \ . \tag{3.1}$$

$q(z) < 0$ corresponds to an accelerating universe, while $q(z) > 0$ means decelerated expansion. By using the definition of the Friedmann equations, as given in the equations (2.3) and (2.4), the deceleration parameter becomes:

$$\begin{aligned} q(z) &= \frac{\frac{\kappa}{2}\left(\rho(z) + 3p(z)\right)}{\kappa\rho(z)} \\ &= \frac{1}{2}[1 + 3\frac{\rho_X}{\rho_m + \rho_X}\frac{p_X}{\rho_X}] \\ &= \frac{1}{2}\left(1 + 3\Omega_X(z)w_X(z)\right) \end{aligned} \tag{3.2}$$

[1] We remark that a simple model with matter as dominant component is out of question for such a behaviour, since it has an equation of state $w_m = 0$. A universe in a phase of accelerated expansion requires a dominant species with an equation of state $w < -1/3$, see equation 3.2.

which restates what we already know: without a dominant species characterized by $w_X < -1/3$, accelerated expansion is not possible. In the following we relate the deceleration parameter q to the distance of supernovae Type Ia, which we infer from the luminosity distance

$$d_L(z) \equiv a_0 r_1 (1+z) \ . \tag{3.3}$$

In this expression r_1 is the comoving coordinate at which light is emitted and a_0 is the scale factor at the present time t_0. On a null geodesic the Robertson-Walker line element (2.1) reduces to

$$dt^2 = a^2 dr^2 \ . \tag{3.4}$$

for a flat universe. Thus, if the light is emitted at t and detected at t_0 by an observer placed at the coordinate $r = 0$, we have

$$r_1 = \int_a^{a_0} \frac{\mathrm{d}a'}{\dot{a}'a'} \tag{3.5}$$

for the comoving coordinate where $a = a(t)$ and $a_0 = a(t_0)$. Inserting this into equation (3.3) yields

$$\begin{aligned} d_L(z) &= a_0 (1+z) \int_a^{a_0} \frac{\mathrm{d}a'}{\dot{a}'a'} \\ &= a_0 (1+z) \int_z^0 -\frac{1}{H(u)a^2} \frac{a_0}{(1+u)^2} \mathrm{d}u \\ &= (1+z) \int_0^z \frac{\mathrm{d}u}{H(u)} \end{aligned} \tag{3.6}$$

where we used the relation $a = a_0 / (1+z)$ to change the integration variable from a to u. This is the standard expression for the luminosity distance [1]. The whole information about the cosmological model considered is encoded in the Hubble parameter H.

In order to relate the luminosity distance d_L to the deceleration parameter q, we have to work out an expression for H. Changing variables in equation (3.1), where we use $\frac{dz}{dt} = -(1+z)$, leads to

$$q = \frac{(1+z)}{H} \frac{\mathrm{d}H}{\mathrm{d}z} - 1 \ . \tag{3.7}$$

By separating variables one obtains

$$\int_{H_0}^{H} \frac{\mathrm{d}H'}{H'} = \int_0^z [q(u) + 1] \frac{\mathrm{d}u}{1+u} \tag{3.8}$$

which, after carrying out the integration, yields an expression for H in terms of the deceleration parameter q. Alternatively, with the help of equation (3.2), we can achieve a dependence on the equation of state w_X of the dark energy:

$$\begin{aligned} H &= H_0 \exp\left(\int_0^z [q(u)+1]\frac{\mathrm{d}u}{1+u}\right) \\ &= H_0 \exp\left(\int_0^z [q(u)+1]\mathrm{d}\ln(1+u)\right) \\ &= H_0 \exp\left(\int_0^z [\frac{3}{2}\left(1+\Omega_X(u)w_X(u)\right)]\mathrm{d}\ln(1+u)\right) \end{aligned} \tag{3.9}$$

where H_0 is the Hubble constant. Inserting the previous equation into equation (3.6) we arrive at

$$d_L = \frac{1+z}{H_0}\int_0^z \mathrm{d}u \exp\left(-\int_0^u [\frac{3}{2}\left(1+\Omega_X(v)w_X(v)\right)]\mathrm{d}\ln(1+v)\right) \quad . \tag{3.10}$$

The whole derivation is valid for a generic dark energy with variable equation of state w_X. In the following, we have to restrict our consideration to cases with $w_X = const$ in order to obtain some quantitative results.[2] We can then use $\rho \propto a^{-3(1+w)}$ (see equation (2.13)) and rewrite Ω_X by considering the ratio between the matter and dark energy density

$$\begin{aligned} \frac{\rho_m}{\rho_X} &= \frac{\rho_m^0}{\rho_X^0}\left(\frac{a}{a_0}\right)^{-3}\left(\frac{a}{a_0}\right)^{3(1+w_X)} \\ &= \frac{\rho_m^0}{\rho_X^0}\left(\frac{a_0}{a}\right)^{3w_X} \quad . \end{aligned} \tag{3.11}$$

As introduced earlier, an index zero always denotes the present day value of a quantity. Using $\rho_m/\rho_X = \Omega_m/\Omega_X$ yields

$$\frac{\Omega_X^0}{\Omega_X} = \frac{\Omega_m^0}{\Omega_m}(1+z)^{-3w_X} \quad . \tag{3.12}$$

For a flat universe $\Omega_m + \Omega_X = 1$ is valid which enables us to find an expression for Ω_X only depending on the redshift:

$$\Omega_X = \left(\frac{\Omega_m^0}{\Omega_X^0}(1+z)^{-3w_X} + 1\right)^{-1} \quad . \tag{3.13}$$

[2] This is not too much of a constraint, since, e.g. for the quintessence models we consider in chapter 4, we can assume that an attractor solution with constant equation of state has been joined long before the transition from deceleration to acceleration occurs.

Inserting the derived expression for Ω_X into equation (3.10) gives

$$d_L = \frac{1+z}{H_0}\int_0^z \mathrm{d}u \exp\left(-\int_0^u [\frac{3}{2}\left(1+w_X\left(\frac{\Omega_m^0}{\Omega_X^0}(1+z)^{-3w_X}+1\right)^{-1}\right)]\mathrm{d}\ln(1+v)\right) \tag{3.14}$$

which, after some algebra, results in

$$d_L = (1+z)H_0^{-1}\left(1+\frac{\Omega_m^0}{\Omega_X^0}\right)^{1/2}\int_0^z du\,\frac{(1+u)^{-3/2}}{\sqrt{\frac{\Omega_m^0}{\Omega_X^0}+(1+u)^{3w_X}}}\,. \tag{3.15}$$

Except for the luminosity distance d_L and the redshift z, which are both measureable quantities, this expression only depends on the equation of state w_X of the dark energy. Equation (3.15) can be integrated for specific values of w_X numerically. The results are presented in figure 3.1 where we chose the values $H_0 = 70\frac{km}{sMpc}$, $\Omega_m^0 = 1/3$ and $\Omega_X^0 = 2/3$. The four curves shown correspond to an equation of state $w_X \in \{-1, -0.5, -0.3, 0\}$ for the dark energy, where the smallest value for w_X belongs to the uppermost curve. The increase in d_L with decreasing w_X at a fixed redshift z is due to the larger acceleration rate. The observational interpretation of this is that supernovae in a universe with smaller w_X are fainter, whereas for larger w_X they are brighter if measured at the same z. As one can see from figure 3.1 the difference between the luminosity distance curves becomes easier to distinguish at larger redshift z. Therefore, the results obtained from observational data at large z will be more significant for our purposes.

3.1.2 Astronomical measurements

Figure 3.2 illustrates the original result of a survey of 42 high redshift Type Ia supernovae which were investigated by the Supernova Cosmology Project [5]. Notice that the data shown are limited up to $z \leq 1$. For the precise discrimination between the different values of w_X measurements at higher redshifts than the ones considered here are required (e.g. $z \gtrsim 2$). Nevertheless, the data shown provide evidence for a phase of recent acceleration in the universe and is consistent with the simplest possibility for a dark energy model: a pure cosmological constant or ΛCDM model.
In the next section we discuss a different method to determine the equation of state w_X quantitatively and derive the redshift z_{acc} at which the acceleration starts for a ΛCDM model.

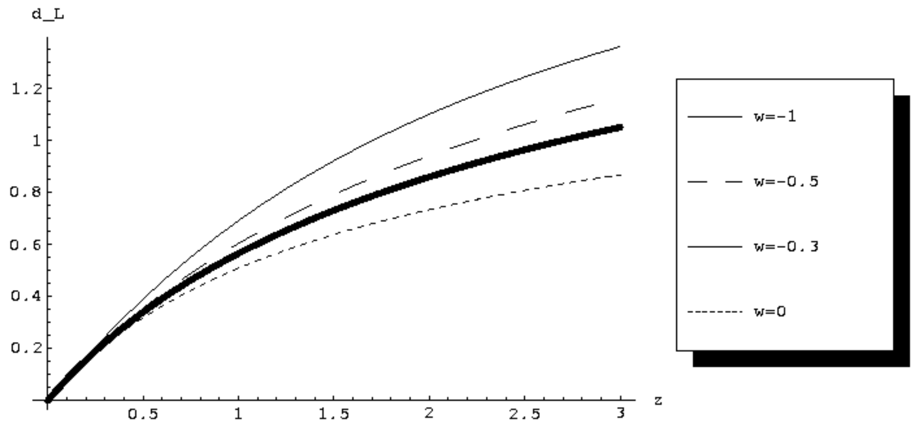

Figure 3.1: Luminosity distance d_L (in $\frac{H_0}{c}$) versus redshift z. The four curves predict how the luminosity distance evolves in a universe with an equation of state $w_X \in \{-1, -0.5, -0.3, 0\}$ of the dark energy.

3.2 Determination of the transition point z_{acc} from deceleration to acceleration

As we have seen in the previous section, supernova Type Ia data favour a universe which undergoes a phase of recent acceleration. However, in order to form structure in the universe we need an early phase of decelerated expansion in which the matter energy density was the dominant component. Thus, there must be a *transition point* z_{acc}, characterized by $q(z_{acc}) = 0$, at which the universe turned from decelerated to accelerated expansion. In this section we examine the dependence of z_{acc} on the equation of state w_X of the dark energy for a flat universe with negligible radiation and compare the results to supernova Type Ia data [5, 6].

3.2.1 Theoretical Predictions

Let us recall equation (3.2) for the deceleration parameter

$$q(z) = \frac{1}{2}\left(1 + 3\Omega_X(z) w_X(z)\right) \ . \tag{3.16}$$

This expression allows us a first interpretation of how the expansion of the universe evolves: Since $\Omega_X \approx 0$ in the early phase of the universe, we have $q > 0$ and hence a deceleration phase. Due to its different decrease with the expansion of the universe the dark energy density becomes the dominant species in the universe and we have $\Omega_X(z) \approx 1$. If $w_X < -1/3$, we enter

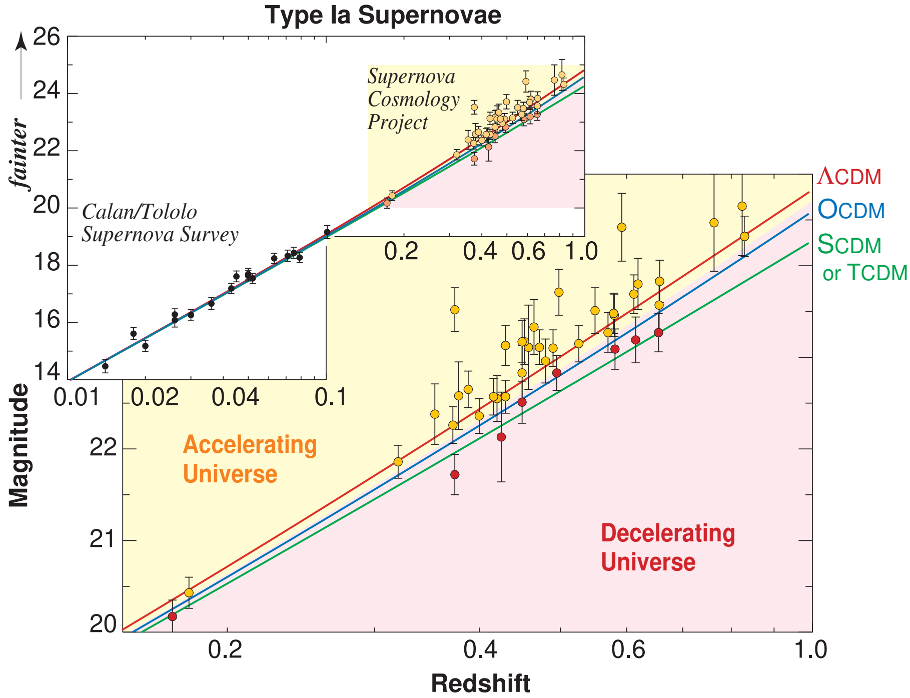

Figure 3.2: Observed brightness (in magnitude) versus redshift z. The observed brightness is inversely proportional to the square of the luminosity distance d_L. The data points at low redshift are taken from the Calan/Tololo Supernova Survey, whereas the data at higher redshift were investigated by the Supernova Cosmology Project [5, 7]. Most of the data points can be found in the yellow area corresponding to an accelerating universe.

a phase of accelerated expansion. Thus the transition from decelerated to accelerated phase is a natural outcome of a cosmological model with a dark energy component of equation of state $w_X < -1/3$. Inserting expression (3.13) for Ω_X into equation (3.16) gives

$$\begin{aligned} q(z) &= \frac{1}{2}[1 + 3w_X \left(\Omega_m^0/\Omega_X^0 \, (1+z)^{-3w_X} + 1\right)^{-1}] \\ &= \frac{1}{2}\left[\frac{\Omega_m^0/\Omega_X^0 \, (1+z)^{-3w_X} + 1 + 3w_X}{\Omega_m^0/\Omega_X^0 \, (1+z)^{-3w_X} + 1}\right] \\ &= \frac{1}{2}\left[\frac{\Omega_X^0/\Omega_m^0 (1+3w_X)\,(1+z)^{3w_X} + 1}{\Omega_X^0/\Omega_m^0 \, (1+z)^{3w_X} + 1}\right] . \end{aligned} \tag{3.17}$$

From this it follows that the transition redshift is to be found at

$$1 + z_{acc} = \left[(1 + 3w_X)(\Omega_m^0 - 1)/\Omega_m^0\right]^{-1/3w_X} \tag{3.18}$$

where we again used that $\Omega_X^0 + \Omega_m^0 = 1$. Solving this equation for Ω_m^0 yields

$$\Omega_m^0 = \frac{1}{1 - (1 + z_{acc})^{-3w_X}/(1 + 3w_X)} \ . \tag{3.19}$$

3.2.2 Astronomical measurements

The result presented in the previous subsection has been compared with observational data from the references [6, 5]. These analyses include observations of supernova Type Ia up to $z \approx 1.7$. By combining (3.19) with supernova Type Ia data we make a statement about which w_X and z_{acc} are favoured. This is done with the help of so-called *confidence contour plots* in the $w_X - \Omega_m^0$ plane. Figure 3.3 is such a plot obtained from measurements of the Supernova Cosmology Project in 1998 [5]. The confidence contours shown restrict the probable values for Ω_m^0 and w_X to a certain region. As can be seen in figure 3.3 cosmological models with $\Omega_m^0 \gtrsim 0.6$ or $w_X \gtrsim -0.3$ are clearly disfavoured by the supernova data.
The combination of the theoretical curves from equation (3.19) and the confidence contour plots is illustrated in figure 3.4. In addition to the contours, the theoretical curves for $z_{acc} \in \{1.0, 1.2, 1.7\}$ are included [6]. Even if we assume $\Omega_m^0 \approx 1/3$ and reject all values outside of the 1σ-area, a large range for w_X is left. In principle values for $-1 \lesssim w_X \lesssim -0.6$ are in agreement with the observational data from figure 3.4. Thus it is reasonable to consider other cosmological models than with a pure cosmological constant.
The same difficulties arise if one examines the range of the transition redshift z_{acc} on the basis of figure 3.4. Since all possible values for z_{acc} intersect with the 1σ-area of the contour plot, we need a reasonable value for Ω_m^0 to decide which z_{acc} is most likely.

In the special case of a universe with vacuum energy (i.e. $w_X = w_\Lambda = -1$) equation (3.18) becomes

$$1 + z_{acc} = \left[2\Omega_\Lambda^0/\Omega_m^0\right]^{1/3} \ . \tag{3.20}$$

For $\Omega_m^0 \approx 1/3$ and $\Omega_\Lambda^0 \approx 2/3$ we obtain

$$z_{acc} \approx 0.59 \ . \tag{3.21}$$

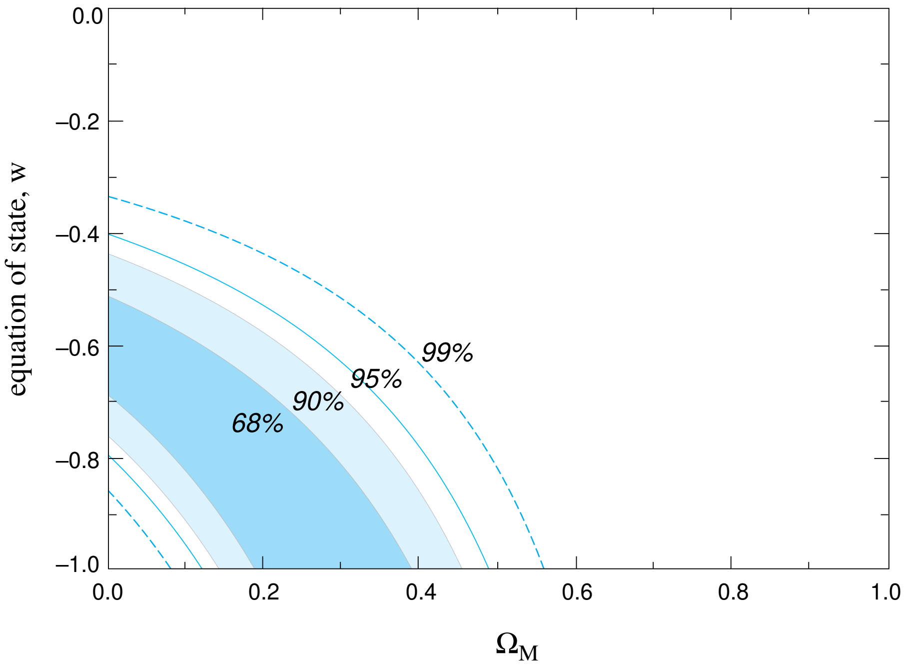

Figure 3.3: Equation of state w_X versus Ω_m^0. The confidence contour plot is the result of supernova Type Ia measurements from the Supernova Cosmology Project in 1998 [5]. The numbers on the contours give the likelihood to find a combination of Ω_m^0 and w_X within the surrounded area. The data reject models with $w_X \gtrsim -0.3$ or $\Omega_m^0 \gtrsim 0.6$.

This is in good agreement with the confidence contour plot 3.4 which favours $z_{acc} \lesssim 1$. So the transition from deceleration to acceleration must have occurred very close to the present epoch if one considers a cosmological constant model.

To conclude the observational data from supernova Type Ia is in agreement with the theory of a cosmological constant and other forms of dark energy with constant equation of state. The confidence contour plots shown do not provide evidence for a certain cosmological model, either. More measurements at higher z are needed in order to determine the equation of state w_X of the dark energy or the transition redshift z_{acc}. The results shown allow us to consider alternative models to a pure cosmological constant model.

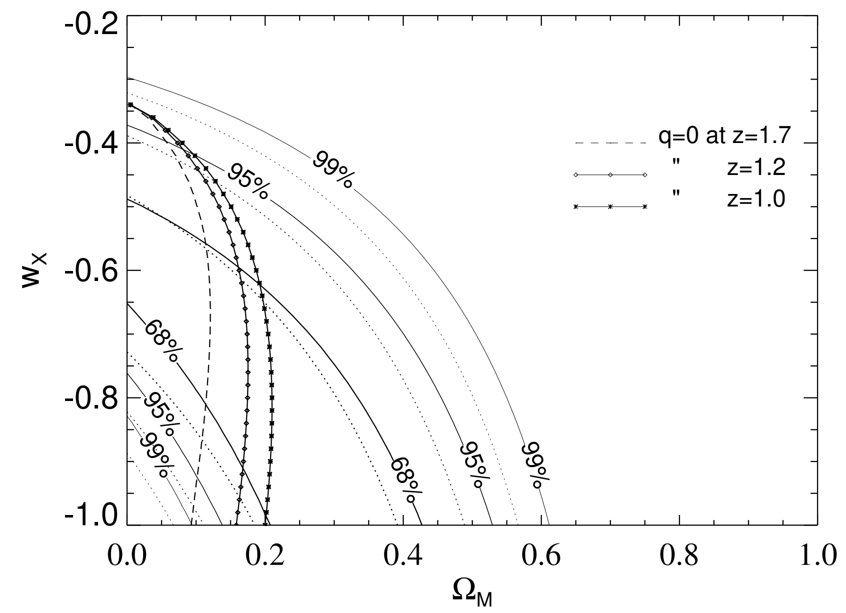

Figure 3.4: Equation of state w_X versus Ω_m^0. This confidence contour plot combines observations from Riess et al. with theoretical curves for different transition redshifts $z_{acc} \in \{1.0, 1.2, 1.7\}$ [6]. If one assumes $\Omega_m^0 \approx 0.3$ models with $w_X \lesssim -0.6$ and $z_{acc} \lesssim 1$ are favoured.

Chapter 4

Quintessence models with tracking behaviour

In order to explain the accelerating phase of the universe at the present time supernova Type Ia measurements suggest the dominance of a dark energy, see e.g. [6, 7]. In the previous chapter we have seen that a cosmological constant as well as other forms of dark energy with an equation of state close to -1 can explain the observational data. Since the cosmological constant model leads to an unnatural scale of the vacuum energy density compared with other particle physics scales and requires a fine-tuning of the initial values, we examine in the following chapters in how far quintessence provides an alternative.
Essentially, the idea of quintessence is to assume the cosmological constant to be zero, e.g. due to a symmetry argument, and to reproduce the observation by taking a sufficiently slowly rolling scalar field. This field then induces a "time varying effective cosmological constant". The motivation of taking a scalar field to describe quintessence is that it offers the simplest realization of a field which is the dominant species and leads to acceleration[1]. In fact the whole dynamics of a homogeneous, time-varying scalar field is well understood from inflation theory and can be applied for quintessence models in a similar way. Since quintessence only weakly interacts with matter, its field should apparently not have a too difficult structure. To avoid the fine-tuning of initial values we restrict the models considered to so-called *tracker fields* [16, 18, 19]. They represent a special class of scalar fields with the property that all solutions to the equation of motion are drawn towards a common attractor.

[1]Alternatively, it is possible to construct quintessence e.g. from topological defects or composite scalars such as fermion condensates. The latter would lead then to an effective model for the universe.

We start in section 4.1 by summarizing the properties of scalar fields and proceed in the subsequent section with the notion of tracker fields. As a result we obtain a tracker criterion which allows us to decide which potentials admit tracking behaviour. Additionally, we study the inverse power law potential $V = M^{\alpha+4}Q^{-\alpha}$ as an example for such a tracker potential and continue in section 4.3 with describing the two possibilities how the energy density of the quintessence field can reach the attractor – namely the *undershoot* and the *overshoot* case. Hereafter, in section 4.4, we impose four constraints a cosmological model should fulfill and apply them to three single field quintessence potentials. We close with the discussion of the fine-tuning of initial values for tracker fields in section 4.5.

4.1 Scalar fields

We consider a spatially homogeneous, time-varying scalar field $Q = Q(t)$ which is described by the Lagrangian density

$$\mathcal{L} = \frac{1}{2}\partial_\mu Q \partial^\mu Q - V(Q) \ . \tag{4.1}$$

The field is assumed to interact with matter and radiation only through gravity. From the action

$$S = \int d^4x \sqrt{-g}\mathcal{L} \tag{4.2}$$

one derives the equation of motion of the scalar field Q for a homogeneous and expanding universe as

$$\ddot{Q} + 3H\dot{Q} + V' = 0 \tag{4.3}$$

where the dots denote time derivatives and the prime a derivative with respect to the field. We recall that the Hubble parameter H is given by

$$H^2 \equiv \left(\frac{\dot{a}}{a}\right)^2 = \kappa\left(\rho_m + \rho_r + \rho_Q\right) \tag{4.4}$$

with $\kappa \equiv \frac{8\pi G}{3}$. The above equations (4.3) and (4.4) contain the complete information on the motion of the scalar field. The stress energy tensor for the Q field is

$$T^{\mu\nu} = \partial^\mu Q \partial^\nu Q - \mathcal{L} g^{\mu\nu} \tag{4.5}$$

where $g^{\mu\nu}$ denotes the metric. Since the tensor has the form of a perfect fluid in this case, the density and the pressure of the scalar field can be identified with

$$\rho_Q = \frac{1}{2}\dot{Q}^2 + V\,, \tag{4.6}$$

$$p_Q = \frac{1}{2}\dot{Q}^2 - V\,. \tag{4.7}$$

Note that the definition of the pressure allows negative values which corresponds to a repulsive force. The equations (4.6) and (4.7) determine the equation of state of the Q-field to be

$$w_Q \equiv \frac{p_Q}{\rho_Q} = \frac{\frac{1}{2}\dot{Q}^2 - V}{\frac{1}{2}\dot{Q}^2 + V}\,. \tag{4.8}$$

From this one can directly see that $-1 \leq w_Q \leq 1$. If the potential of the Q-field is much larger than the kinetic energy term we have $w_Q \simeq -1$. If the kinetic energy term dominates we have $w_Q \simeq 1$ instead.

4.2 Tracker fields

4.2.1 The tracker criterion

In this thesis we work with a special type of potentials $V = V(Q)$ for the scalar field Q, the so-called *tracker potentials*, which were originally proposed by Zlatev, Steinhardt and Wang [16, 18, 19]. These potentials have the property that they provide a *tracker solution* $\tilde{Q} = \tilde{Q}(t)$ to the equation of motion (4.3) to which all other solutions $Q = Q(t)$ converge[2] within in a large range of inital values. By *tracker solution* we mean an attractor to which all solutions of the equation of motion are drawn and which has an approximately constant equation of state $w_{\tilde{Q}}$. If a potential has tracking behaviour the corresponding scalar fields are denoted as *tracker fields.*
During most of the evolution (where the tracking properties are actually discussed) the scalar field Q is assumed to have a negligible energy density ρ_Q compared with some other form of energy which is controlling the expansion

[2]In the following we will often use the word *tracking* instead of *converging*. While the expression "converging" corresponds to the typical behaviour of a solution which approaches the attractor the whole time, "tracking" allows the solution to behave arbitrarily during short intervals. The converging property of solutions could e.g. be lost during matter-radiation equality. However, this slight difference can often be ignored. Therefore we use the two expressions interchangeable.

of the universe. We generically denote this dominating field as the *background field* and call its equation of state w_B. Typically, this is either radiation ($w_B = 1/3$) or matter ($w_B = 0$). Only at late times, the energy density of Q dominates.

Tracker fields have the property that a very wide range of initial conditions leads to a common cosmological track with an equation of state $w_{\tilde{Q}} = w_{\tilde{Q}}(w_B)$. As a consequence the ultimate evolution of the universe will be determined by the potential V, while being rather insensitive to the initial conditions for the field Q.

We are interested in tracker solutions whose equation of states $w_{\tilde{Q}}$ are (i) *approximately constant* (i.e. $\dot{w}_{\tilde{Q}} \approx 0$) and (ii) *satisfying* $w_{\tilde{Q}} \neq -1$. In this case it is possible to give a criterion to determine whether a potential admits a tracker solution with the above properties. Therefore, we introduce the quantity

$$\Gamma \equiv \frac{V'' \, V}{(V')^2} \; . \tag{4.9}$$

We will say that Γ is nearly constant if it satisfies

$$\frac{\Gamma'/\Gamma}{V'/V} \ll 1 \; . \tag{4.10}$$

As we show in appendix A, a potential V(Q) has tracking behaviour with the two properties (i) and (ii) given above, if Γ is nearly constant and if

$$\Gamma > \hat{\Gamma} \equiv 1 - \frac{1 - w_B}{6 + 2\, w_B} \tag{4.11}$$

where w_B is the equation of state of the background. We will refer to the above inequality as the *tracker criterion*[3].

In appendix A, we have also shown that if the tracker criterion is satisfied the equation of state $w_{\tilde{Q}}$ of the tracking solution is related to the one of the background by

$$w_{\tilde{Q}} \approx \frac{w_B - 2\;(\Gamma - 1)}{1 + [2\;(\Gamma - 1)]} \, , \qquad \dot{w}_{\tilde{Q}} \approx 0 \; . \tag{4.12}$$

In order to have the Q-field overtake the background at late times, one must have $w_Q \leq w_B$. In this case equation (4.12) requires $\Gamma \geq 1$, which indeed satisfies $\Gamma > \hat{\Gamma}$ (provided that $w_B < 1$, see equation (4.11)). Note that, once the tracker solution is dominant (i.e. $w_{\tilde{Q}} = w_B$), equation (4.12) rewrites as

[3] The criterion that we have stated ensures the existence of an attractor solution $\tilde{Q}$. The proof (given in appendix (A.4)) consists of showing that solutions Q which at some point of time are close enough to $\tilde{Q}$ directly converge to it.

$(\Gamma - 1)w_{\tilde{Q}} \approx -(\Gamma - 1)$. Therefore in all models with $\Gamma > 1$, $w_{\tilde{Q}}$ will finally become -1.
The advantage of the criterion just stated is that we can determine the tracking behaviour of a given potential without having to solve the equation of motion (4.3) , since the quantity Γ is given only in terms of V and its derivatives.

4.2.2 Example for a tracker potential

So far we have introduced several expressions and equations for tracker potentials. Let us now consider the inverse power law potential as an illustrating example

$$V(Q) = M^{4+\alpha}Q^{-\alpha} \tag{4.13}$$

where M and α are constants. This family of potentials was originally studied by Ratra and Peebles [13]. From the given potential we have:

$$V' = -\alpha\frac{M^{4+\alpha}}{Q^{\alpha+1}} \ , \quad V'' = \alpha(\alpha+1)\frac{M^{4+\alpha}}{Q^{\alpha+2}} \tag{4.14}$$

so that, from equation (4.9),

$$\Gamma = 1 + \frac{1}{\alpha} \ . \tag{4.15}$$

Notice that Γ is independent of Q. Furthermore, for $\alpha > 0$ one has $\Gamma \geq 1$. Thus, according to the tracker criterion, the potential $V(Q) = M^{4+\alpha}Q^{-\alpha}$ admits a tracker solution. In this specific case equation (4.12), relating the equation of state of the Q-field to the one of the background, rewrites

$$w_{\tilde{Q}} \approx \frac{\alpha\, w_B - 2}{\alpha + 2} \ . \tag{4.16}$$

4.3 Evolution of the energy density

In general, solutions $Q(t)$ of the equation of motion (4.3) can approach the attractor $\tilde{Q}(t)$ in two different ways as illustrated in figure 4.1. We distinguish between the *overshoot case*, which is characterized by $\frac{1}{2}\dot{Q}_i^{\,2} \gg |V_i|$, and the *undershoot case*, which corresponds to $\frac{1}{2}\dot{Q}_i^{\,2} \ll |V_i|$. The subscript i always denotes the initial value of the variable.

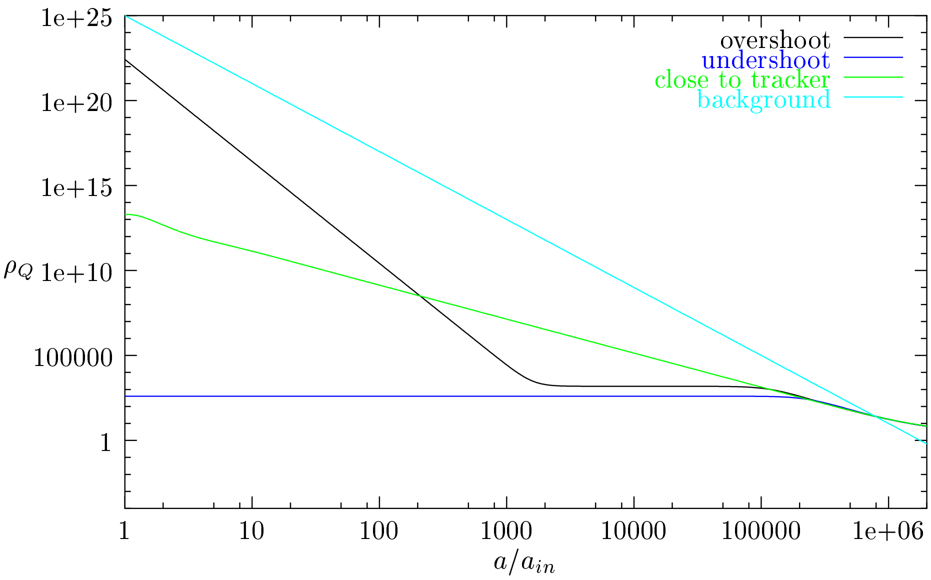

Figure 4.1: Energy density (in arbitrary units) versus scale factor (normalized to a_{in}) for the evolution of a tracker field with the potential $V(Q) = M^6 Q^{-2}$. The overshoot case was generated with initial values $Q_i = 5 \cdot 10^{-4}$ and $\dot{Q}_i = 0.025$; whereas for the undershoot we chose $Q_i = 0.05$ and $\dot{Q}_i = 0$. Both join the attractor rather late whereas the solution with initial values $Q_i = 2.25 \cdot 10^{-7}$ and $\dot{Q}_i = 0$ ends on the track almost immediately.

The overshoot case starts with a stage of kinetic energy domination in which we can neglect the potential energy of the Q-field[4]. Since $\rho_{Q_i} \approx p_{Q_i} \approx \frac{1}{2}\dot{Q}_i^2$ we see from equation (4.8) that the equation of state of the quintessence field has the value $w_{Q_i} \approx 1$. Hence the field dissipates its kinetic energy with $\rho_Q \sim a^{-3(1+w_Q)} \sim a^{-6}$. In this stage the quintessence energy density drops down much faster than the one of the background as can be seen in figure 4.1. When $\dot{Q} \approx 0$ the quintessence field freezes at a value Q_f. This description enables us to give an approximation for the value Q_f[5]:

$$Q_f \approx Q_i + \sqrt{\frac{2\rho_{Q_i}}{H_i^2}} \tag{4.17}$$

[4]Typically, one takes $\rho_{Q_i} < \rho_{B_i}$ in order to have a reasonable behaviour of the quintessence energy density at the present time (see section 4.4, *hierarchy constraint*).

[5]The derivation of the equation for Q_f is given in appendix B.

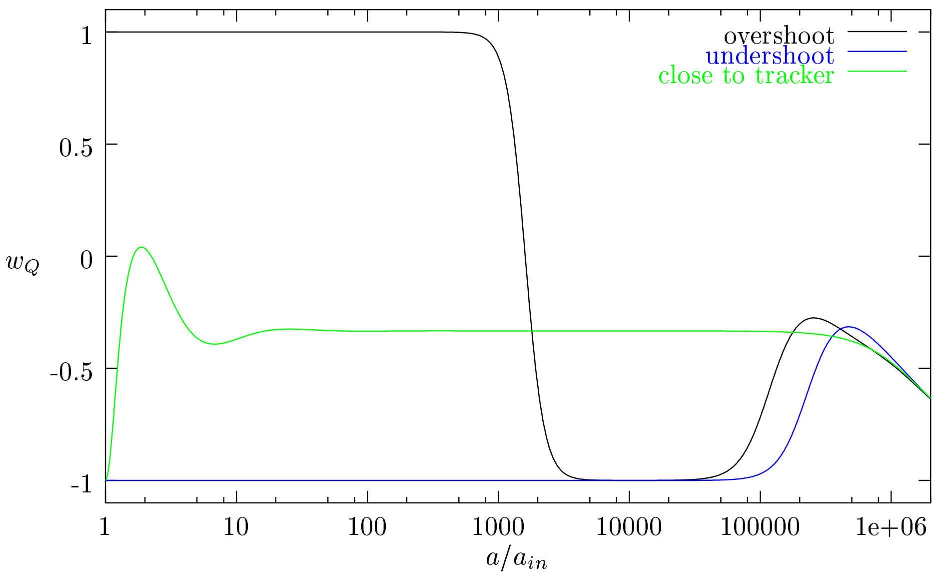

Figure 4.2: Equation of state versus scale factor (normalized to a_{in}) for the same potential $V(Q) = M^6 Q^{-2}$. The illustrated energy densities have the same initial values as in figure 4.1.

assuming $\rho_{Q_i} < \rho_{B_i}$. As one can see from equation (4.17) the value at which the Q-field freezes depends on Q_i, $\dot{Q}_i$ and the initial energy density ρ_{B_i}.
Notice that the characteristic behaviour of the tracker field in this *kinetic energy* regime and the value Q_f are independent of the potential V. The scaling is due to the domination of the kinetic energy term, whereas the duration of this regime depends only on the initial value of the kinetic energy. After the Q-field has dissipated its kinetic energy in the overshoot case, the energy density ρ_Q evolves only due to the potential energy and one is left with $\rho_Q \approx -p_Q \approx V$.
In the undershoot case the first stage is skipped, since it directly starts with $\rho_{Q_i} \approx V_i$ (see figure 4.1). From this point on the two cases undergo the same evolution. Since the potential energy dominates, we have $w_Q \approx -1$ (see equation (4.8)). Consequently, the Q-field and its energy density stay approximately constant and cannot be distinguished from a cosmological constant at this stage. The stage where Q and ρ_Q are frozen is called the *slow roll* regime and holds as long as we have $m^2 = |V''| < H^2$ (*slow roll condition*). The tracking behaviour is now important for the further evolution of the field. It insures that the solutions join the attractor in this regime if they have not done it before.

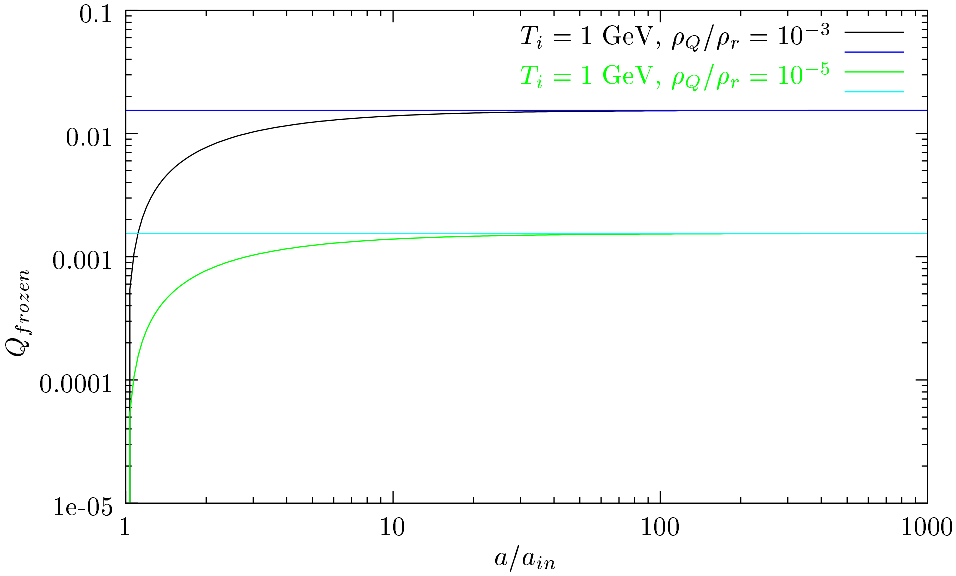

Figure 4.3: Q (in arbitrary units) versus the scale factor a (normalized to a_{in}). The two straight lines are calculated from equation (4.17) whereas the solid and the dashed curve correspond to the evolution of Q according to the numerical simulations.

In order to show the different behaviour of the two cases mentioned above we have integrated the equations of motion for Q and for the scale factor a numerically.[6] Then, we have illustrated in figure 4.1 the evolution of the quintessence energy density of three different solutions. One of them is close to the tracker solution since very early times while the other two are in the overshoot and undershoot regime. The parameters chosen have no relevance for cosmology; the only purpose of figure 4.1 is to point out the characteristics of the two different behaviours which – as we have noticed – occurs quite generally for different tracker potentials.
To confirm the results of our approximation for Q_f we compared the calculated value from equation (4.17) with our numerical simulation of the evolution of Q. Figure 4.3 shows how the numerical value of the field Q approaches the estimated one for two different initial $\dot{Q}_i$. Indeed in comparison with the whole evolution until the present time both values for Q_f are reached after a short time. As expected the solution with larger initial $\dot{Q}_i$ freezes at a larger value of Q_f. This justifies working with the approximation (4.17) during the subsequent sections.

[6] Details of the numerical integrations are given in appendix C.

4.4 Cosmological constraints for quintessence

In this section we discuss the constraints imposed on several types of potentials by various cosmological considerations. All potentials should fulfill the following constraints:

1. One would like to begin with $\rho_{Q_i} < \rho_{B_i}$ but not $\rho_{Q_i} \ll \rho_{B_i}$ in order not to introduce a too big hierarchy between the two different forms of energy. An initial condition ρ_{Q_i} may be a natural outcome at the end of inflation assuming that the energy density of the inflaton is equipartitioned between the various degrees of freedom (*hierarchy constraint*).

2. It is preferable to have a model where Q starts rolling somewhat before the present epoch, otherwise a nearly constant ρ_Q would not be distinguishable from a pure cosmological constant (*unique behaviour*).

3. The Q-field should dominate the universe at the present epoch in order to show measurable effects (*late time domination*).

4. To have accelerated expansion in the universe $w_Q < -1/3$ is required. Observations (see chapter 3) even indicate that $w_Q < -0.6$ (*accelerated expansion*).

4.4.1 The potential $V(Q) = \hat{V} e^{-\tilde{\lambda} Q/M_P}$

We consider the exponential potential $V(Q) = \hat{V} e^{-\tilde{\lambda} Q/M_P}$. Since $\Gamma = 1$ for this type of potential, the tracker criterion (4.11) is fulfilled and equation (4.12) yields $w_{\tilde{Q}} \approx w_B$. Thus the energy density of the scalar field $\rho_{\tilde{Q}}$ scales like the one of the background ρ_B and the ratio between $\Omega_{\tilde{Q}}$ and Ω_B is constant. If the tracker solution is joined before or during matter domination this potential does not lead to accelerated expansion around the present time. But it is also possible to tune the model in such a way that the attractor is reached only recently at a redshift $z \approx 1$. We discuss this issue in more details in chapter 5.

4.4.2 The potential $V(Q) = M^{4+\alpha} Q^{-\alpha}$

As we have already seen in the previous section the inverse power law potential $V(Q) = M^{4+\alpha} Q^{-\alpha}$ admits tracking behaviour for all real $\alpha > 0$.
From the *unique behaviour* constraint, we are able to give a lower bound for the exponent α of the inverse power law potential (see reference [16]). The

more observational requirements give us an upper bound for α since they restrict the equation of state of the tracker solution to $w_{\tilde{Q}} < -0.5$.
In order to give a lower bound for α we have to find an inequality in which all other quantities can be determined by measurements. Assuming equipartition after inflation, it is natural to start in the overshoot case, with $\Omega_{Q_i} \sim 10^{-3} \gg \Omega_{\tilde{Q}_i}$. Then, the field Q quickly evolves from the initial value Q_i to a value Q_f, characterized by $\Omega_{Q_f} \ll \Omega_{\tilde{Q}_i}$, where it freezes. As long as Q is frozen, Ω_Q increases with respect to $\Omega_{\tilde{Q}}$. When the two quantities become equal, Q starts evolving along the attractor solution $\tilde{Q}$. For the latter, we have $\sqrt{\frac{\Omega_{\tilde{Q}}}{\kappa}} \sim V/V'$ (see section A.2). Using the fact that Q is frozen at Q_f, Ω_Q can be estimated as

$$\Omega_Q \approx \frac{V}{\rho_{crit}} \propto \frac{\kappa V}{H^2} \; . \tag{4.18}$$

By setting $\Omega_Q = \Omega_{\tilde{Q}}$, we can determine the value of the Hubble parameter H_{roll} when Q starts evolving along the tracker solution

$$\frac{\kappa V}{H_{roll}^2} = \frac{\kappa V^2}{V'^2} \Rightarrow H_{roll}^2 = \frac{V'^2}{V} \; . \tag{4.19}$$

We demand that this evolution started at latest at the time of matter-radiation equality. Thus, denoting by H_{eq} the value of the Hubble parameter at matter-radiation equality, we require

$$\left.\frac{V'^2}{V}\right|_{Q=Q_f} \geq H_{eq}^2 \; . \tag{4.20}$$

In order to evaluate the quantity H_{eq}, we consider the ratio between H_{eq} and the present value of the Hubble rate H_0. Since most of the evolution of H in this period occurred during the matter dominated era, we have

$$H_{eq}^2 = \frac{H_0^2}{a_{eq}^3} \; , \tag{4.21}$$

where we set $a_0 = 1$ and used the fact that $a \propto t^{2/3} \propto H^{-2/3}$ during the matter dominated era. Combining equations (4.20) and (4.21) we have

$$\left.\frac{V'^2}{V}\right|_{Q=Q_f} \geq \frac{H_0^2}{a_{eq}^3} \; . \tag{4.22}$$

In this regime equation (4.18) is a good approximation for the value of Ω_Q^0. Thus, equation (4.22) can be rewritten as

$$\left.\frac{V'^2}{V}\right|_{Q=Q_f} \geq \frac{\kappa V_0}{\Omega_Q^0 a_{eq}^3} \ . \tag{4.23}$$

By specializing to the power law potential $V(Q) = M^{4+\alpha} Q^{-\alpha}$, the last inequality can be expressed in the form

$$\frac{\alpha^2}{Q_f^{\alpha+2}} \geq \frac{\kappa}{Q_0^\alpha \Omega_Q^0 a_{eq}^3} \ . \tag{4.24}$$

To obtain a lower bound on α the two quantities Q_f and Q_0 must be determined. Since $\Omega_Q^0 = \Omega_{\tilde{Q}}$ and the Q-field varies only slightly at the present epoch, we can apply the equations (4.18) and (4.19) in order to estimate Q_0:

$$\frac{V_0'^2}{V_0} \approx H_0^2 \approx \kappa \frac{V_0}{\Omega_Q^0} \tag{4.25}$$

which gives

$$Q_0^2 \approx \frac{1}{\kappa} \Omega_Q^0 \alpha^2 \tag{4.26}$$

for the inverse power law potential. Since $\rho_{Q_i} < \rho_{B_i}$ initially, we can take equation (4.17) to estimate the frozen value Q_f (see appendix B for further details of the calculation). With $Q_i \ll M_P$ this is

$$Q_f \approx \sqrt{\frac{2}{\kappa} \Omega_{Q_i}} \ . \tag{4.27}$$

Inserting the last two expressions into equation (4.24) gives

$$\alpha^2 \geq \frac{\kappa \left(\frac{1}{2\kappa} \Omega_{Q_i}\right)^{1+\alpha/2}}{\left(\frac{1}{\kappa} \Omega_Q^0 \alpha^2\right)^{\alpha/2} \Omega_Q^0 a_{eq}^3} \tag{4.28}$$

and with $a_{eq} \sim 10^{-4}$, $\Omega_{Q_i} \sim 10^{-3}$ and $\Omega_Q^0 \approx 2/3$ we obtain

$$\alpha^{2+\alpha} \gtrsim 10^{12} \frac{10^{-3(1+\alpha/2)}}{10^{-\alpha/2}} \tag{4.29}$$

which gives approximately the following lower bound

$$\alpha \geq 5 \; . \tag{4.30}$$

So, if we assume the *hierarchy constraint* and the *unique behaviour* as stated at the beginning of this chapter, we obtain a lower bound for α in case of the inverse power law potential.
Unfortunately, values of $\alpha \geq 5$ are incompatible with the other requirements that we want to impose. If the energy density of the Q-field should dominate at late times we need the potential V to increase as Q is increasing and therefore small values of the power law exponent α. If we would like the universe to accelerate at the present epoch we obtain an upper bound for α. Requiring $w_Q = -\frac{1}{3}$ in order to have an accelerated expansion yields $\alpha < 4$ for matter domination (i.e. with $w_B = 0$ in equation (4.16)). If we also take the observational constraints on $w_Q < -0.5$ into account equation (4.16) gives $\alpha < 2$.
To conclude, the inverse power law potential $V(Q) = M^{4+\alpha}Q^{-\alpha}$ fails to fulfill all requirements in our scenario of the universe. Thus it cannot be considered as a successfull model for quintessence.

4.4.3 The potential $V(Q) = M^4 e^{M_P/Q}$

A better choice with regard to the constraints mentioned in the beginning of the chapter is the potential $V(Q) = M^4 e^{M_P/Q}$ (see [16]). Let us first verify the tracking behaviour of the potential by applying the tracker criterion (4.11). With the help of equation (4.10) we find

$$\frac{\Gamma'/\Gamma}{V'/V} = -\frac{2}{\frac{M_P^2}{Q^2} + \frac{2M_P}{Q}} \ll 1 \tag{4.31}$$

if $Q \ll M_P$. Thus Γ can be considered as approximately constant in this case. Since equation (4.9) yields

$$\Gamma = 1 + \frac{2Q}{M_P} \; , \tag{4.32}$$

which fulfills $\Gamma > 1$ for $Q > 0$, the potential admits tracking behaviour.
We can now Taylor expand the potential in a series of inverse power laws. This has the advantage, in comparison with the previous case, that different powers $(Q/M_P)^{-\alpha}$ dominate the universe at different times. At early times we have $Q \ll M_P$ and large values of the power law exponent α are dominating,

so that the Q-field starts to roll at an appropriate time. At late times the terms with small α dominate instead and thus w_Q is negative today. In this way it is possible to satisfy all the requirements that are stated in the beginning of the chapter.

4.5 Fine-tuning of the initial values

Let us consider a potential V which admits a tracker solution and fulfills the four constraints stated in the previous section. Since the property of tracker fields is that a wide range of solutions of the equation of motion finally joins the attractor, we would like to discuss in this section how many of these solutions lead to a *reasonable cosmological model*. Or, in other words, how much *fine-tuning* is involved in order to end up with a universe where ρ_Q and ρ_m are of the same order at the present time[7]?

If we consider, e.g., the pure cosmological constant case, it is obvious that only one initial value ρ_{Λ_i} leads to a universe with exactly $\Omega_\Lambda^0 = 2/3$ and $\Omega_m^0 = 1/3$ and thus we can tolerate only a small interval of initial values ρ_{Λ_i} in order to have a reasonable model.

For quintessence models with tracking behaviour we have to advance in two steps: First we have to scale the tracker potential such that $\rho_{\tilde{Q}}$ and ρ_m are of the same order today. Strictly speaking, this is a fine-tuning itself, but on a scale that is more natural compared with fundamental scales. Once the parameters of the potential are fixed, we determine the bounds of the interval $[\rho_{Q_i}^{min}; \rho_{Q_i}^{max}]$ for the allowed initial ρ_{Q_i} which show the same behaviour as the attractor.

Let us assume that for the model to work the tracker solution should be joined before matter-radiation equality. The lower bound $\rho_{Q_i}^{min}$ can then be found by considering the undershoot case which reaches the attractor exactly at the time t_{eq} of equality (see figure 4.4). In this case one obtains the lower bound easily from evaluating

$$\rho_{Q_i}^{min} = \rho_B(t_{eq}) = \rho_B^0 z_{eq}^3 \ , \tag{4.33}$$

[7] This issue is often denoted as *coincidence problem*, see e.g. [16, 18, 19].

where ρ_B^0 denotes the present value of the background. In analogy, the upper bound $\rho_{Q_i}^{max}$ can be determined by finding the appropriate overshoot case which freezes at $\rho_{Q_i}^{min}$ (see figure 4.4). More precisely, we have to use equation (4.17) to set up the equation

$$V(Q_f) = \rho_B^0 z_{eq}^3 \qquad \text{with} \quad Q_f \simeq \sqrt{\frac{2\rho_{Q_i}^{max}}{H_i}} \tag{4.34}$$

and solve for $\rho_{Q_i}^{max}$. All other $\rho_{Q_i} \in [\rho_{Q_i}^{min}; \rho_{Q_i}^{max}]$ can be identified either with an undershoot or an overshoot case joining the attractor before matter-radiation equality. As examples for this a typical undershoot and a slight overshoot are illustrated in figure 4.4. Since we consider a logarithmic scale the total range of the initial values $\rho_{Q_i}^{max} - \rho_{Q_i}^{min}$ is much larger than in the pure cosmological constant case.

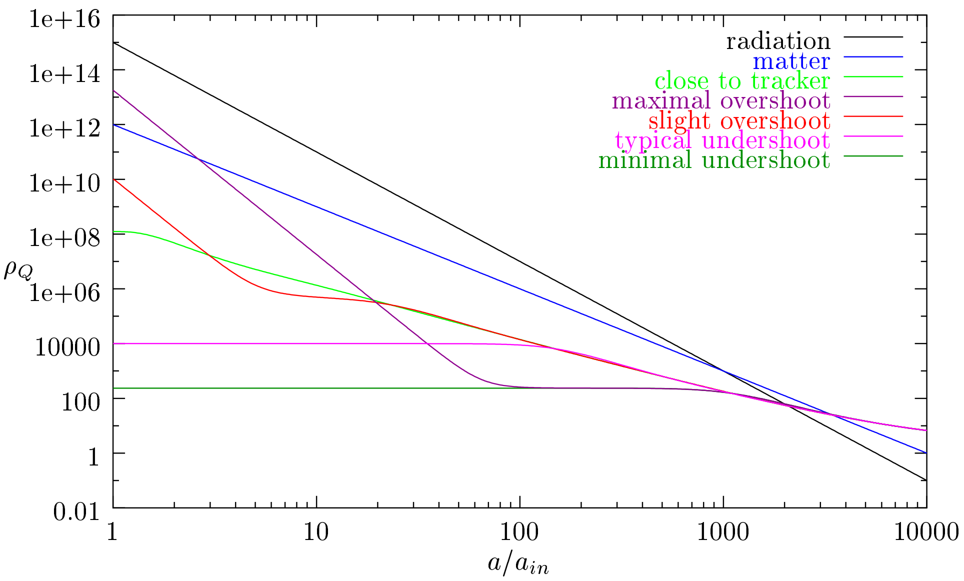

Figure 4.4: Energy density (in arbitrary units) versus scale factor (normalized to a_{in}) for the evolution of a tracker field with the potential $V(Q) = M^6 Q^{-2}$. The initial values for radiation and matter were chosen in such a way that matter-radiation-equality is at $a/a_{in} = 1000$.

All this confirms the advantage of quintessence models with tracker potentials in comparison with a cosmological constant model. Although we have to restrict the initial values in the sense that they lead to a reasonable cosmological model[8], there is still a large range for the interval $[\rho_{Q_i}^{min}; \rho_{Q_i}^{max}]$ left. In our specific example of the inverse power law potential in figure 4.4 we have a range of more than 10 orders of magnitude.

[8]In our scenario we require e.g. that all solutions of the equation of motion have joined the tracker solution at latest at matter-radiation equality.

Chapter 5

Quintessence models with an exponential potential

In this chapter we discuss a model in which the accelerating phase is long enough to explain the supernova data [6, 7], but has a finite duration in order to be consistent with string theory [23, 24]. The model is characterized by an exponential potential [20, 21]

$$V = \hat{V}\, e^{-\tilde{\lambda} Q/M_P}, \quad \tilde{\lambda} \equiv \sqrt{8\pi}\lambda \tag{5.1}$$

which we have already studied as a toy model for quintessence with tracking behaviour in subsection 4.4.1. We have seen that this potential leads to a model with tracking behaviour where the energy density of the tracker solution $\tilde{Q}$ scales exactly like the one of the background ($w_{\tilde{Q}} \approx w_B$). In particular, we discuss the case in which the Q-field has reached the tracker solution $\tilde{Q}$ which evolves like an effective matter energy density. By choosing the initial values in an appropriate way we are able to generate a phase of accelerated expansion that starts at the present epoch, before reaching the attractor $\tilde{Q}$ at some point in the future (see figure 5.1).
The underlying idea is to take a field Q that is essentially frozen at a value Q_f during most of the evolution of the universe. This is due to the friction term $3H\dot{Q}$ provided by the expansion of the universe in the equation of motion $\ddot{Q} + 3H\dot{Q} + V' = 0$ of the scalar field Q. As long as the effective mass $m = \sqrt{d^2V/dQ^2}$ of the Q-field is smaller than the Hubble parameter H, the field is in a regime of slow roll. Since the Hubble parameter H decreases with time, the field starts to roll at a certain time. By choosing the initial values of the field Q such that $\sqrt{V''(Q_f)} \approx H_0$, where the zero denotes the present value of the Hubble parameter, one can make sure that the field rolls at the present epoch[1]. The energy density ρ_Q then overtakes the background

[1] In this chapter *present* means at very recent time, $z \simeq 1$, as compared to the whole

energy density ρ_B and becomes the dominant species in the universe. This is a necessary condition in order to have an accelerating phase at recent times. Basically, there are two possibilities to construct a model in this way. The first one is to choose the initial conditions so that the kinetic energy density can be neglected (*undershoot case*). The field Q is then frozen from the beginning and the redshift at which the accelerated phase starts is determined by the initial value of the field Q_i. Alternatively, one can choose an initial value ρ_{Q_i} in which the kinetic energy term dominates (*overshoot case*). As a consequence, the field Q first undergoes a stage in which all the kinetic energy density is dissipated. During this regime the energy density of the Q-field drops down much faster than the one of the background. When $\dot{Q} \approx 0$ the field Q freezes and it evolves as described for the undershoot case. In contrast to the undershoot case here the choice of the initial velocity $\dot{Q}_i$ determines the point of time at which the accelerated phase starts.
In the following we discuss in more details how the energy density ρ_Q evolves for the two cases mentioned above. Section 5.1 summarizes the tracking properties of the exponential potential. In section 5.2 we discuss the slow roll regime and how the transition from background to quintessence domination occurs. From the slow roll condition we are able to calculate the ratio between background and quintessence energy density at the time at which the roll starts. In this way we can find the dependence of the redshift z_{acc} at which this occurs on the initial energy density ρ_{Q_i}. Finally, in section 5.3 we study the amount of fine-tuning that is necessary to fit the supernova results and compare it to standard quintessence models as discussed in chapter 4.

5.1 The tracking properties of the exponential potential

The tracking behaviour of the potential defined by equation (5.1) depends on the choice of the parameter λ. One distinguishes between three cases [20, 15]:

- $\lambda^2 \leq 3$:

  In this case we have no tracking behaviour neither in the radiation dominated nor in the matter dominated regime.

- $3 < \lambda^2 < 4$:

  Within this range of λ the energy density of the quintessence field tracks only in the matter dominated phase.

---

history of the universe.

- $\lambda^2 \geq 4$:

  In this case we obtain tracking solutions during both regimes.

If an attractor solution exists, the following property of the energy density of the $\tilde{Q}$-field is valid [15]:

$$\Omega_{\tilde{Q}} \equiv \frac{\rho_{\tilde{Q}}}{\rho_{crit}} = \frac{3}{\lambda^2}(1 + w_B) \ , \tag{5.2}$$

where w_B is the equation of state of the background. This expression can be rewritten as the ratio between the energy density of the $\tilde{Q}$-field and the one of the background

$$\frac{\rho_{\tilde{Q}}}{\rho_B} = \frac{\frac{3}{\lambda^2}(1 + w_B)}{1 - \frac{3}{\lambda^2}(1 + w_B)} \ . \tag{5.3}$$

Specializing to a matter dominated universe ($w_B = 0$) and considering the range of λ with tracking only in the matter dominated phase, we have $3 \leq \frac{\rho_{\tilde{Q}}}{\rho_B} < \infty$. As one can see from equation (5.3), the ratio $\frac{\rho_{\tilde{Q}}}{\rho_B}$ only depends on the value of the parameter λ. Therefore the Q-field scales in the same way as matter ($w_Q = 0$) once the attractor is reached.

5.2 The slow roll regime and the accelerated phase

As we have seen in chapter 4, section 4.3, the early evolution of the quintessence energy density in general occurs independent of the considered potential V. Indeed, figure 5.1 shows the typical evolution of a tracker field in the overshoot case. Thus we start the discussion of the evolution of the exponential potential with the *slow roll* regime, where the field Q and the energy density ρ_Q are frozen. For the exponential potential (5.1) with

$$V'' = \frac{8\pi\lambda^2}{M_P^2}V, \quad H^2 = \frac{8\pi}{3}\frac{\rho_B + \rho_Q}{M_P^2} \ , \tag{5.4}$$

the *slow roll* condition (see chapter 4, section 4.3) corresponds to the following ratio between the background and the quintessence energy density:

$$m^2 = |V''| < H^2 \Leftrightarrow \frac{\rho_{B_s}}{\rho_{Q_s}} > 3\lambda^2 - 1 \ . \tag{5.5}$$

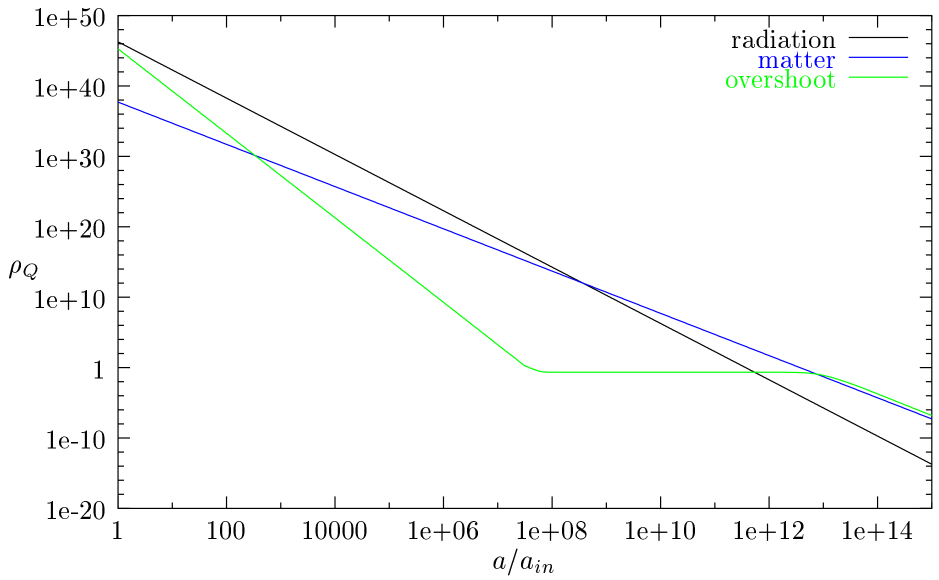

Figure 5.1: Energy density (in arbitrary units) versus scale factor (normalized to a_{in}) for the potential $V(Q) = e^{-10Q/M_P}$. The illustrated overshoot solution has the initial values $Q_i = 0$ and $\rho_{r_i}/\rho_{Q_i} = 0.1$. The background starts evolving from an initial temperature $T_i = 1\text{GeV}$.

Since λ^2 varies between 3 and 4 in the parameter space that we are considering, we have

$$\frac{\rho_{B_s}}{\rho_{Q_s}} \in [8; 11] \tag{5.6}$$

at the point where the slow roll stage ends and the Q-field starts to roll again. As one can see from the previous equation (5.6) the background energy density is still dominant when the roll starts but of the same order as ρ_Q. Figure 5.2 – which was obtained from numerical simulations – is in agreement with this statement. While the equation of state of the Q-field w_Q increases the corresponding energy density ρ_Q overtakes the background and becomes the dominant species. As long as the quintessence field is dominant and has an equation of state $w_Q < -1/3$ the universe is in an accelerated phase. However, since we have chosen the Q-field to track the matter energy density this accelerated phase is rather short. Finally, the attractor solution with $w_{\tilde{Q}} = 0$ is reached and ρ_Q/ρ_B stays constant at a value only depending on λ (see equation (5.3)).
The accelerated stage is the crucial point of the model, since the duration of

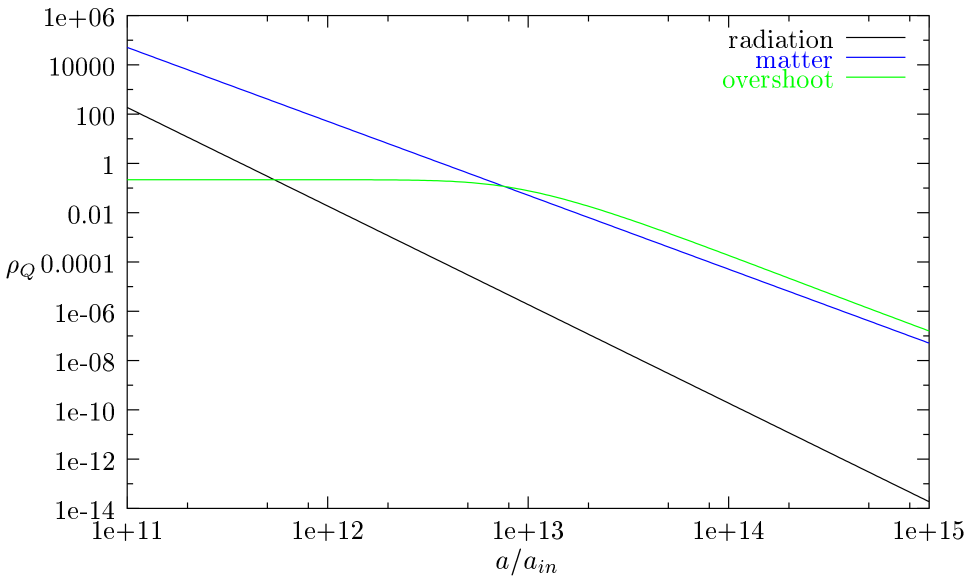

Figure 5.2: Energy density (in arbitrary units) versus scale factor (normalized to a_{in}) for the potential $V(Q) = e^{-10Q/M_P}$. The initial values are the same as in figure 5.1.

the acceleration and the redshift z_{acc} at which the acceleration[2] starts must be in agreement with the supernova data. Since the Q-field freezes before matter-radiation equality for the cases in which the model works, we can set the initial time of our numerical simulations at matter-radiation equality in this section. At best the acceleration starts at z_{acc} and ends today at z_0 where $w_Q = -1/3$, so that we can observe the whole period of acceleration. Clearly, $\Delta z \equiv z_{acc} - z_0$ then gives us the duration of the accelerated phase as well as the point of time at which the universe turns from decelerated to accelerated expansion (see figure 5.2).

To calculate how ρ_{Q_i} depends on the redshift z_{acc}, we consider how the background energy density evolves

$$\rho_B = \begin{cases} \rho_m^0 (1+z)^3, & z < z_{eq} \\ \rho_m^0 \frac{(1+z)^4}{(1+z_{eq})}, & z > z_{eq} \end{cases} \tag{5.7}$$

[2]With good accuracy the redshift at which the acceleration starts is the same as the redshift at which the quintessence energy density begins to dominate.

where ρ_m^0 denotes the present value of the matter energy density. At equality of matter and quintessence energy density we have

$$\rho_Q^{acc} = \rho_m^{acc} = \rho_m^0 \left(1 + z_{acc}\right)^3 \ . \tag{5.8}$$

Hence one obtains

$$z_{acc} = \sqrt[3]{\frac{\rho_Q^{acc}}{\rho_m^0}} - 1 \ . \tag{5.9}$$

Since the Q-field is still in the slow roll regime when it is in the vicinity of the background energy density, one approximates ρ_Q^{acc} by ρ_{Q_f}. In the undershoot case this is simply ρ_{Q_i}. For the overshoot case one can neglect the kinetic energy term in the energy density to obtain ρ_{Q_f}, but has to take into account the previous stage of kinetic energy domination. Thus one has

$$\rho_{Q_f} \approx \hat{V} e^{-\tilde{\lambda} Q_f / M_P} \tag{5.10}$$

which, combined with equation (4.17), leads to

$$\rho_{Q_f} \approx \hat{V} e^{-\tilde{\lambda}\sqrt{\frac{2\rho_{Q_i}}{H_i^2}}/M_P} \ . \tag{5.11}$$

Notice that in equation (4.17) we normalized to $Q_i = 0$, since a change in Q_i corresponds to rescaling the parameter $\hat{V}$. Inserting this into equation (5.9) we end up with the following expression for the redshift z_{acc}:

$$z_{acc} = \begin{cases} \sqrt[3]{\frac{\rho_{Q_i}}{\rho_m^0}} - 1, & \text{for the undershoot case} \\ \sqrt[3]{\frac{\hat{V} e^{-\tilde{\lambda}\sqrt{2\rho_{Q_i}}/H_i M_P}}{\rho_m^0}} - 1, & \text{for the overshoot case} \end{cases} \tag{5.12}$$

In the next section we will check the plausibility of the model by discussing which range for ρ_{Q_i} is consistent with the supernova observations.

5.3 The fine-tuning of the initial conditions for the exponential potential

As for standard quintessence models we would now like to investigate the coincidence problem. Since the attractor solution cannot explain the present situation of an accelerating universe we have to ensure that quintessence

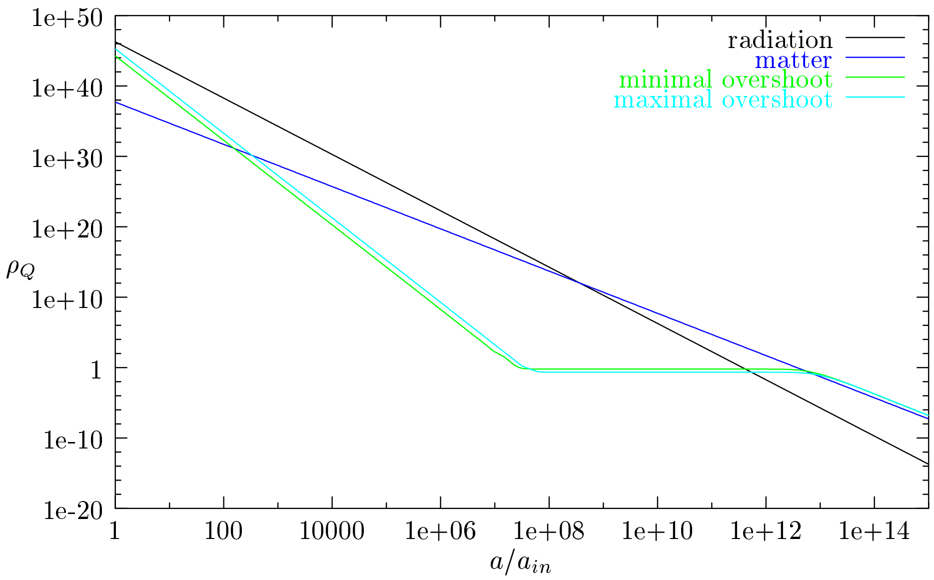

Figure 5.3: Energy density (in arbitrary units) versus scale factor (normalized to a_{in}) for the potential $V(Q) = e^{-10Q/M_P}$. Restricting our consideration to overshoot solutions, only the initial values between the maximal and minimal overshoot lead to a model with acceleration at the present time.

becomes dominant before joining the attractor at the present epoch. In the last section we analysed the dependence of the initial value of the energy density ρ_{Q_i} on the redshift z_{acc} at which the universe starts to accelerate. Let us assume that the acceleration starts in the range $z_{acc} \in [1; 2]$ and find out in which interval for ρ_{Q_i} we end up for the undershoot and the overshoot case. We choose $z_{acc} \in [1; 2]$ in order to be consistent with observational constraints. As we have seen from the supernova Type Ia observations (see chapter 3) the dark energy component has to become the dominant species when z_{acc} is of the order 1 to explain the new phase of acceleration in the universe. If we then relate the length of the interval of ρ_{Q_i} to the initial background energy density ρ_{B_i} we find the amount of *fine-tuning* that is necessary in order to obtain a reasonable cosmological model for the various cases.

5.3.1 The undershoot case

From equation (5.12) we know that in the undershoot case

$$\rho_{Q_i} = \rho_m^0 \left(z_{acc} + 1\right)^3 \tag{5.13}$$

holds. Thus $z_{acc} \in [1, 2]$ corresponds to $\rho_{Q_i} \in [8\rho_m^0, 27\rho_m^0]$. If we relate this interval to the initial background energy density[3] ρ_{B_i}, as given in equation (5.7), we obtain

$$\frac{\Delta\rho_{Q_i}}{\rho_{B_i}} \simeq \frac{20(1 + z_{eq})}{(1 + z_{in})^4} , \tag{5.14}$$

where z_{in} denotes the redshift of the universe at the initial time. If z_{in} is large – which is equivalent to an older universe – the fraction $\frac{\Delta\rho_{Q_i}}{\rho_{B_i}}$ has to be smaller respectively. Hence, the longer the period of radiation domination considered the more we have to fine-tune the initial ρ_{Q_i} in order to end up at a reasonable value for z_{acc}. The amount of fine-tuning required is the same as for a cosmological constant.

5.3.2 The overshoot case

In the overshoot case the initial energy density of the quintessence field is given as

$$\rho_{Q_i} = \frac{H_i^2 M_P^2}{2\tilde{\lambda}} \left(\ln(\frac{\hat{V}}{\rho_m^0}(1 + z_{acc})^{-3})^2 \right) , \tag{5.15}$$

as follows from equation (5.12). In analogy to the undershoot case, we are interested in the range of ρ_{Q_i} that corresponds to $z_{acc} \in [1, 2]$. With these bounds we have

$$\Delta\rho_{Q_i} = \frac{H_i^2 M_P^2}{2\tilde{\lambda}} \left((\ln \frac{\hat{V}}{8\rho_m^0})^2 - (\ln \frac{\hat{V}}{27\rho_m^0})^2 \right) , \tag{5.16}$$

where we can choose $\hat{V} = k\rho_m^0$ where k is of order 1. With $H_i^2 \approx \kappa\rho_{B_i}$ the relative range of the ρ_{Q_i} interval is

$$\frac{\Delta\rho_{Q_i}}{\rho_{B_i}} = \frac{2\pi}{3\tilde{\lambda}} \left((\ln \frac{k}{8})^2 - (\ln \frac{k}{27})^2 \right) \tag{5.17}$$

[3] This is a reasonable scale for the relative difference, since a priori $\rho_{Q_i} \lesssim \rho_{B_i}$ is valid. The approximate equality is satisfied if one has e.g. equipartition after inflation.

which is independent of the redshift z_{in}. This is an advantage with respect to what we found above, since – contrary to the undershoot case – the allowed interval $\frac{\Delta\rho_{Q_i}}{\rho_{B_i}}$ does not become smaller as we increase z_{in}. Figure 5.3 illustrates how close upper and lower bound for the initial ρ_{Q_i} have to be in the overshoot case in order to achieve the present acceleration for $z \in [1; 2]$.
Compared with pure tracking quintessence models, both cases fail to improve the solution of the fine-tuning problem. For the standard quintessence potentials (see chapter 4) a much wider range of initial conditions is allowed, since there it is enough to require that the field Q joins the attractor at any redshift between z_{in} and $z \sim 1$.

Chapter 6

Conclusion

In this thesis, we showed that the tracker criterion is a powerful tool to analyse the tracking behaviour of quintessence models with scalar fields. We have seen that the evolution occurs in general independently of the potential chosen and leads to one cosmological track.
Furthermore, we investigated under which circumstances the exponential, the inverse power law and the inverse exponential potential fulfill the necessary cosmological constraints for a realistic model. Standard quintessence models are able to explain the current accelerated phase of the universe. Alternative quintessence models with an exponential potential have this property as well. We discussed in detail the sensitivity to initial conditions of both models. Standard quintessence models are insensitive to initial values and solve in this sense the coincidence problem. The exponential potential has a finite duration of the acceleration phase. Hence, we have to fine-tune the range of possible initial values more carefully. This is an advantage to a cosmological constant model but cannot solve the coincidence problem in the same way as pure tracker quintessence models can.
Additionally, we analysed the supernova Type Ia measurements. From confidence contour plots we were able to restrict the equation of state of the dark energy to $w_X \lesssim -0.6$ and saw that the acceleration has to start at a redshift $z \simeq 1$. From these measurements, we can infer that a dark energy component is present, but we cannot make a definite statement on its nature. For this, measurements of supernovae at higher redshifts would be needed.

Appendix A

Basic equations for tracker potentials

In this appendix we derive the tracker criterion which ensures that a given potential V has a tracker solution $\tilde{Q}(t)$. Since the attractor is characterized by a constant equation of state $w_{\tilde{Q}}$, we can additionally give a relation between the tracker potential V, the background w_B and the equation of state $w_{\tilde{Q}}$. The proof for the tracker criterion consists of showing that solutions which are initially close to $\tilde{Q}(t)$ directly converge to it. That is, starting from the solution $Q(t_i) \equiv \tilde{Q}\ (t_i) + \Delta(t_i)$ characterized by $\Delta(t_i) \ll Q(t_i)$ at some initial time t_i, one can show analytically that $\Delta(t)$ rapidly goes to zero for $t > t_i$. Numerical simulations suggest that – if the tracker criterion is satisfied – solutions within a very wide range of initial conditions (i.e. with $\Delta(t_i)$ not necessarily small) converge to $\tilde{Q}(t)$.

A.1 The equation of motion

Our aim is to give a criterion whether a potential V admits tracking solutions without explicitly solving the equation of motion (4.3). To do so we introduce the following quantities:

$$\begin{aligned}
V' &\equiv \frac{\mathrm{d}V}{\mathrm{d}Q} \\
1+w_Q &= \frac{\frac{1}{2}\dot{Q}^2+V}{\frac{1}{2}\dot{Q}^2+V} + \frac{\frac{1}{2}\dot{Q}^2-V}{\frac{1}{2}\dot{Q}^2+V} = \frac{\dot{Q}^2}{\rho_Q} \\
x &\equiv \frac{1+w_Q}{1-w_Q} = \left(\frac{\dot{Q}^2}{\frac{1}{2}\dot{Q}^2+V}\right)\left(\frac{\frac{1}{2}\dot{Q}^2+V}{2V}\right) = \frac{\frac{1}{2}\dot{Q}^2}{V}
\end{aligned} \tag{A.1}$$

$$\begin{aligned}
\dot{x} &\equiv \frac{\mathrm{d}\ln x}{\mathrm{d}\ln a} = \frac{\mathrm{d}\ln x}{\mathrm{d}t}\frac{a}{\dot{a}} = \frac{\mathrm{d}\ln\frac{1}{2}\dot{Q}^2/V}{\mathrm{d}t}\frac{1}{H} \\
&= \frac{V}{\frac{1}{2}\dot{Q}^2}\frac{\mathrm{d}\frac{1}{2}\dot{Q}^2/V}{\mathrm{d}t}\frac{1}{H} = \frac{V}{\frac{1}{2}\dot{Q}^2}\frac{\dot{Q}\ddot{Q}V-\frac{1}{2}\dot{Q}^2V'\dot{Q}}{V^2}\frac{1}{H} \\
&= \frac{2}{\dot{Q}}\frac{\ddot{Q}V-\frac{1}{2}\dot{Q}^2V'}{V}\frac{1}{H}
\end{aligned}$$

so that

$$1+\frac{1}{6}\dot{x} = \frac{3\dot{Q}\,VH+\ddot{Q}V-\frac{1}{2}\dot{Q}^2V'}{3\,\dot{Q}\,VH}\ . \tag{A.2}$$

Starting with equation (4.3) one finds:

$$
\begin{aligned}
& \ddot{Q} + 3H\dot{Q} + V' = 0 \\
\Leftrightarrow \quad & \ddot{Q}V + 3H\dot{Q}V + V'V = 0 \\
\Leftrightarrow \quad & \ddot{Q}V + 3H\dot{Q}V - \frac{1}{2}\dot{Q}^2V' + \frac{1}{2}\dot{Q}^2V' + V'V = 0 \\
\Leftrightarrow \quad & \ddot{Q}V + 3H\dot{Q}V - \frac{1}{2}\dot{Q}^2V' + V'\left(\frac{1}{2}\dot{Q}^2 + V\right) = 0 \\
\overset{(4.6)}{\Leftrightarrow} \quad & \ddot{Q}V + 3H\dot{Q}V - \frac{1}{2}\dot{Q}^2V' + V'\rho_Q = 0 \\
\Leftrightarrow \quad & \frac{\ddot{Q}V + 3H\dot{Q}V - \frac{1}{2}\dot{Q}^2V'}{V} = -\frac{V'\rho_Q}{V} \\
\Leftrightarrow \quad & \frac{3\dot{Q}H}{\rho_Q}\frac{\ddot{Q}V + 3H\dot{Q}V - \frac{1}{2}\dot{Q}^2V'}{3\dot{Q}HV} = -\frac{V'}{V} \\
\overset{(A.2)}{\Leftrightarrow} \quad & \frac{3\dot{Q}H}{\rho_Q}\left(1 + \frac{1}{6}\dot{x}\right) = -\frac{V'}{V} \qquad \text{(A.3)} \\
\Rightarrow \quad & 3\sqrt{\frac{\dot{Q}^2H^2}{\rho_Q^2}}\left(1 + \frac{1}{6}\dot{x}\right) = \pm\frac{V'}{V} \\
\Leftrightarrow \quad & 3\sqrt{\frac{H^2\kappa}{\rho_Q\kappa}}\sqrt{1+w_Q}\left(1 + \frac{1}{6}\dot{x}\right) = \pm\frac{V'}{V} \\
\overset{(A.1)}{\Leftrightarrow} \quad & \boxed{\pm\tfrac{V'}{V} = 3\sqrt{\tfrac{\kappa}{\Omega_Q}}\sqrt{1+w_Q}\left(1 + \tfrac{1}{6}\tfrac{d\ln x}{d\ln a}\right)}\,. \qquad \text{(A.4)}
\end{aligned}
$$

Notice that $\dot{Q}$ can be positive or negative; therefore one has to be careful when putting $\dot{Q}$ under the square root. The $+$ sign on the left hand side of equation (A.4) is valid for $V' > 0$, while the $-$ sign is valid for $V' < 0$. This expression is an alternative way to write the equation of motion.

A.2 The tracker condition

The tracking solution $\tilde{Q}(t)$ (see section 4.2.1) has the property that $w_{\tilde{Q}}$ is nearly constant and lies between w_B and -1. For $1 + w_Q = \mathcal{O}(1)$ one has $\frac{1}{2}\dot{Q}^2 \sim V \sim \frac{\rho_Q}{2}$. Since $\rho_Q = \frac{\rho_Q}{\rho_c}\rho_c = \Omega_Q\frac{H^2}{\kappa}$ it follows that $\dot{Q}^2\kappa \approx \Omega_Q H^2$. Thus, for a tracker solution, equation (A.4) simplifies to

$$\frac{V'}{V} \approx \sqrt{\frac{\kappa}{\Omega_Q}} \approx \frac{H}{\dot{Q}}\,. \qquad \text{(A.5)}$$

We can take this approximation as a condition of whether a solution to the equation of motion is on the track. For this reason equation (A.5) will be called the *tracker condition.*
It is also possible to express the tracker condition in terms of w_Q. For this, we rearrange equation (A.4) as follows:

$$\begin{aligned} \frac{1}{6}\frac{d\,\ln x}{d\,\ln a} &= -\frac{1}{3\sqrt{\kappa(1+w_Q)}}\sqrt{\Omega_Q}\frac{V'}{V}-1 \\ &\equiv \Delta(t)-1\,. \end{aligned} \tag{A.6}$$

If the tracker condition is fulfilled, this expression should be approximately equal to zero. By using $x \equiv (1+w_Q)/(1-w_Q)$, we can rewrite equation (A.6) in terms of w_Q:

$$\tag{A.7}$$

$$\begin{aligned} \frac{1}{6}\frac{d\,\ln x}{d\,\ln a} &= \frac{1}{6}\frac{d\,\ln\frac{1+w_Q}{1-w_Q}}{d\,t}\frac{1}{H} \\ &= \frac{1}{6}\frac{1-w_Q}{1+w_Q}\frac{\mathrm{d}}{\mathrm{d}t}\left(\frac{1+w_Q}{1-w_Q}\right)\frac{1}{H} \\ &= \frac{1}{6}\frac{1-w_Q}{1+w_Q}\frac{\dot{w}_Q(1-w_Q+1+w_Q)}{(1-w_Q)^2} \\ &= \frac{1}{3(1-w_Q^2)}\,\dot{w}_Q \end{aligned} \tag{A.8}$$

where the dot denotes a derivative with respect to $\ln a$.

$$\tag{A.9}$$

From this we see that the tracker condition (A.5) is equivalent to the two conditions: (i) $1-w_Q^2$ significantly different from zero and (ii) w_Q nearly constant.

A.3 The tracker equation

Let us now consider the quantity

$$\Gamma \equiv \frac{V''V}{(V')^2}\,. \tag{A.10}$$

By taking the derivative of V'/V one finds

$$\frac{\mathrm{d}}{\mathrm{d}Q}\frac{V'}{V} = \frac{V''\,V}{V^2} - \frac{V'^2}{V^2}$$

so that

$$\frac{V^2}{V'^2}\frac{\mathrm{d}}{\mathrm{d}Q}\frac{V'}{V} = \frac{V''\,V}{V'^2} - 1$$

and Γ rewrites to

$$\Gamma \equiv \frac{V''V}{(V')^2} = \frac{V^2}{V'^2}\frac{\mathrm{d}}{\mathrm{d}Q}\frac{V'}{V} + 1\,. \tag{A.11}$$

To give a more explicit expression for Γ we consider the case $V' < 0$ and split equation (A.4) into two expressions:

$$\begin{aligned}
\frac{\mathrm{d}}{\mathrm{d}Q}\frac{V'}{V} &= \frac{\mathrm{d}}{\mathrm{d}Q}\left(\underbrace{-3\sqrt{\frac{\kappa}{\Omega_Q}}\sqrt{1+w_Q}}_{A}\underbrace{\left(1+\frac{1}{6}\frac{d\,\ln x}{d\,\ln a}\right)}_{B}\right) \\
&= \frac{\mathrm{d}}{\mathrm{d}Q}(-\,A\,B\,) \equiv -A'\,B\,-\,A\,B' \\
\Rightarrow \Gamma &= \frac{V^2}{V'^2}(-A'\,B\,-\,A\,B') + 1 \\
&= -\frac{A'}{A^2B} - \frac{B'}{AB^2} + 1\ .
\end{aligned}$$

For the calculation it is useful to derive some intermediate results. We first define

$$\dot{x} \equiv \frac{\mathrm{d}\ln x}{\mathrm{d}\ln a} = \frac{1}{H}\frac{\mathrm{d}x}{\mathrm{d}t}\ , \tag{A.12}$$

$$\ddot{x} \equiv \frac{d^2\ln x}{d(\ln a)^2} = \frac{\mathrm{d}\dot{x}}{\mathrm{d}\ln a} = \frac{\mathrm{d}\dot{x}}{\mathrm{d}t}\frac{\mathrm{d}t}{\mathrm{d}\ln a} = \frac{1}{H}\frac{\mathrm{d}\dot{x}}{\mathrm{d}t} \tag{A.13}$$

and write the Friedmann equation (2.3) as

$$H^2 = \kappa(\rho_Q + \rho_B) = \kappa\rho_{crit} \tag{A.14}$$

where ρ_B is the dominant species which is either ρ_m or ρ_r. The time derivative of the last expression yields

$$\begin{aligned}
2H\dot{H} &= \kappa(\dot{\rho}_Q + \dot{\rho}_B) \\
2H\dot{H} &= \kappa\,(-3H)\,((1+w_B)\rho_B + (1+w_B)\rho_Q) \\
\dot{H} &= -\frac{3}{2}\kappa\,(\rho_B + \rho_Q + w_B\rho_B + w_Q\rho_Q) \\
\dot{H} &= -\frac{3}{2}\kappa\,(\rho_{crit} + w_B(\rho_B + \rho_Q) + \rho_Q(w_Q - w_B)) \\
\dot{H} &= -\frac{3}{2}\kappa\left(\frac{H^2}{\kappa} + w_B\frac{H^2}{\kappa} + \rho_Q(w_Q - w_Q)\right) \\
\dot{H} &= -\frac{3}{2}\left((1+w_B)H^2 + \kappa\rho_Q(w_Q - w_B)\right)\,. \qquad \text{(A.15)}
\end{aligned}$$

With

$$\begin{aligned}
A &= 3\sqrt{\frac{\kappa}{\Omega_Q}}\sqrt{1+w_Q} \\
&= 3\sqrt{\frac{\kappa\rho_{crit}}{\rho_Q}}\sqrt{1+\frac{\frac{1}{2}\dot{Q}^2 - V}{\frac{1}{2}\dot{Q}^2 + V}} \\
&= 3\sqrt{\frac{\kappa H^2}{\kappa\rho_Q}}\sqrt{\frac{\dot{Q}^2}{\frac{1}{2}\dot{Q}^2 + V}} \\
&= 3\sqrt{\frac{H^2}{\rho_Q}}\sqrt{\frac{\dot{Q}^2}{\rho_Q}} = \frac{3H\dot{Q}}{\rho_q} \qquad \text{(A.16)}
\end{aligned}$$

the first denominator in equation (A.11) is

$$\begin{aligned}
A^2B &= \frac{9H^2\dot{Q}^2}{\rho_Q^2}(1+\frac{1}{6}\dot{x}) \\
&= \frac{9H^2(1+w_Q)}{\rho_Q}\frac{1}{6}(6+\dot{x}) \\
&= \frac{\frac{3}{2}H^2(1+w_Q)(6+\dot{x})}{\rho_Q} \\
&= \frac{3}{4}\frac{H^2}{\rho_Q}\,2(1+w_Q)(6+\dot{x})\,. \qquad \text{(A.17)}
\end{aligned}$$

Calculating

$$
\begin{aligned}
B' &= \frac{\mathrm{d}}{\mathrm{d}Q}\left(\frac{1}{6}(6+\dot{x})\right) = \frac{1}{6\dot{Q}}\frac{\mathrm{d}}{\mathrm{d}t}(6+\dot{x}) \\
&= \frac{1}{6\dot{Q}}\frac{\mathrm{d}}{\mathrm{d}t}\dot{x} = \frac{1}{6}\frac{H}{\dot{Q}}\ddot{x} \qquad \text{(A.18)}
\end{aligned}
$$

leads to the first term of Γ:

$$
\begin{aligned}
-\frac{B'}{B^2A} &= \frac{-\frac{1}{6}\frac{H}{\dot{Q}}\ddot{x}}{\frac{1}{6^2}(6+\dot{x})^2\,\frac{3H\dot{Q}}{\rho_q}} = -\frac{2\ddot{x}}{\frac{\ddot{Q}}{\rho_q}\,(6+\dot{x})^2} \\
&= -\frac{2\ddot{x}}{(1+w_Q)(6+\dot{x})^2}\,. \qquad \text{(A.19)}
\end{aligned}
$$

Taking A as in the last line of (A.16) we have

$$
\begin{aligned}
A' &= 3\frac{\mathrm{d}}{\mathrm{d}Q}\left(\frac{H\dot{Q}}{\rho_Q}\right) = 3\frac{1}{\dot{Q}}\frac{\mathrm{d}}{\mathrm{d}t}\left(\frac{H\dot{Q}}{\rho_Q}\right) \\
&= \frac{3}{\dot{Q}}\left(\frac{\dot{H}\dot{Q}}{\rho_Q} + H\frac{\mathrm{d}}{\mathrm{d}t}\frac{\dot{Q}}{\rho_Q}\right) = \frac{3}{\dot{Q}}\left(\frac{\dot{H}\dot{Q}}{\rho_Q} + H\frac{\ddot{Q}\rho_Q - \dot{Q}\dot{\rho_Q}}{\rho_Q^2}\right) \\
&= \frac{3}{\dot{Q}\rho_Q}\left(\dot{H}\dot{Q} + H\ddot{Q} + 3H^2\dot{Q}(1+w_Q)\right)
\end{aligned}
$$

and inserting $\dot{H}$ from equation (A.15) gives

$$\begin{aligned}
A' &= \frac{3}{\rho_Q}\left(\dot{H} + 3H^2(1+w_Q)\right) + \frac{3H\ddot{Q}}{\dot{Q}\rho_Q} \\
&= \frac{3}{\rho_Q}\left(-\frac{3}{2}\left(H^2(1+w_B) + \kappa\rho_Q(w_Q - w_B)\right) + 3H^2(1+w_Q)\right) \\
&\quad + \frac{3H\ddot{Q}}{\dot{Q}\rho_Q} \\
&= \frac{9}{2\rho_Q}H^2\left(-1 - w_B + 2 + w_Q\right) + 3\kappa(w_Q - w_B) + \frac{3H\ddot{Q}}{\dot{Q}\rho_Q} \\
&= \frac{9}{2\rho_Q}H^2\left(1 - w_B + w_Q\right) + 3\kappa(w_Q - w_B) + \frac{3H\left(-3H\dot{Q} - V'\right)}{\dot{Q}\rho_Q} \\
&= \frac{9}{2\rho_Q}H^2\left(1 - w_B + w_Q\right) + 3\kappa(w_Q - w_B) - \frac{9H^2}{\rho_Q} - \frac{3HV'}{\dot{Q}\rho_Q} \\
&= \frac{9}{2\rho_Q}H^2\left(-1 - w_B + w_Q\right) + 3\kappa(w_Q - w_B) - \frac{3HV'}{\dot{Q}\rho_Q} \\
&= \frac{9}{2\rho_Q}H^2\left(-1 - w_B + w_Q\right) + 3\kappa(w_Q - w_B) + \frac{3H^2V}{2\rho_Q^2}(6+\dot{x})
\end{aligned}$$

where we have used from equation (A.3)

$$-\frac{V'}{V} = \frac{3\dot{Q}H}{6\rho_Q}(6+\dot{x}) \Leftrightarrow -\frac{3H}{\dot{Q}\rho_Q}V' = \frac{3H^2V}{2\rho_Q^2}(6+\dot{x}) \tag{A.20}$$

to eliminate the term proportional to V'.

$$\tag{A.21}$$

We can now give an expression for the second term in Γ:

$$
\begin{aligned}
-\frac{A'}{AB} &= \frac{\frac{9}{2\rho_Q}H^2\left(-1-w_B+w_Q\right)+3\kappa(w_Q-w_B)+\frac{3H^2V}{2\rho_Q^2}(6+\dot{x})}{\frac{3}{4}\frac{H^2}{\rho_Q}\underbrace{2(1+w_Q)(6+\dot{x})}_{T}} \\
&= -\frac{6(-1-w_B+2w_Q)}{T}-\underbrace{\frac{4\kappa\rho_Q(w_Q-w_B)}{H^2T}}_{S}-2\frac{V}{\rho_Q}\frac{1}{2(1+w_Q)} \\
&= -\frac{\dot{x}\left(1+w_B-2w_Q\right)}{T}+\frac{(6+\dot{x})(1+w_B-2w_Q)}{T}-S-2\frac{V}{\rho_Q}\frac{1}{2(1+w_Q)} \\
&= -\frac{\dot{x}\left(1+w_B-2w_Q\right)}{T}+\frac{w_B-w_Q}{2(1+w_Q)}+\frac{1-w_Q}{2(1+w_Q)}-2\frac{V}{\rho_Q}\frac{1}{2(1+w_Q)}-S \\
&= -\frac{\dot{x}\left(1+w_B-2w_Q\right)}{T}+\frac{w_B-w_Q}{2(1+w_Q)}+\frac{\frac{\rho_Q-p_Q}{\rho_Q}}{2(1+w_B)}-2\frac{V}{\rho_Q}\frac{1}{2(1+w_Q)}-S \\
&= -\frac{\dot{x}\left(1+w_B-2w_Q\right)}{T}+\frac{w_B-w_Q}{2(1+w_Q)}+\frac{\frac{1}{2}\dot{Q}^2+V-\frac{1}{2}\dot{Q}^2+V}{2(1+w_B)}-2\frac{V}{\rho_Q}\frac{1}{2(1+w_Q)}-S \\
&= -\frac{\dot{x}\left(1+w_B-2w_Q\right)}{T}+\frac{w_B-w_Q}{2(1+w_Q)}-S \\
&\approx -\frac{\dot{x}\left(1+w_B-2w_Q\right)}{2(1+w_Q)(6+\dot{x})}+\frac{w_B-w_Q}{2(1+w_Q)}\,. \qquad \text{(A.22)}
\end{aligned}
$$

It is reasonable to neglect S, since the expression

$$
S=-\frac{4\kappa\rho_Q}{H^2T}(w_Q-w_B)=\frac{-4\Omega_Q(w_Q-w_B)}{T}=\frac{4\Omega_Q(w_B-w_Q)}{T}
$$

is much smaller than the other terms. To see this explicitly we compare S to the second term of equation (A.22):

$$
\frac{w_B-w_Q}{2(1+w_Q)}+\frac{4\Omega_Q(w_B-w_Q)}{2(1+w_Q)(6+\dot{x})}=\frac{w_B-w_Q}{2(1+w_Q)}\left(1+\frac{8\Omega_Q}{(6+\dot{x})}\right)\,.
$$

Since $\dot{x}\approx 0$ and $\Omega_B \gg \Omega_Q$, in this regime, we see that S can indeed safely be neglected.

From all this we see that solutions of the equation of motion are characterized by the *tracker equation*

$$
\begin{aligned}
\Gamma &\equiv \frac{V''V}{(V')^2} \\
&= 1 + \frac{w_B - w_Q}{2(1+w_Q)} - \frac{1 + w_B - 2w_Q}{2(1+w_Q)} \frac{\dot{x}}{6+\dot{x}} - \frac{2}{(1+w_Q)} \frac{\ddot{x}}{(6+\dot{x})^2}
\end{aligned}
\tag{A.23}
$$

where we recall that $\dot{x} \equiv d\,\ln x/d\,\ln a$ and $\ddot{x} \equiv d^2\,\ln x/d\,(\ln a)^2$.

A.4 A criterion for tracking behaviour

So far we have found a condition of whether a generic solution of the equation of motion (A.4) is a tracker solution. In addition we have introduced a function Γ which only depends on the potential V of the Q-field and its derivatives with respect to Q.
Our present aim is to find a criterion whether tracker solutions are stable, i.e. whether they are attractors of the solution $Q(t)$ of the equation of motion (A.4). This criterion will be determined by the properties of Γ.
For the criterion to work it is required that Γ is approximately constant which means that

$$
\Gamma^{-1} \frac{1}{H} \frac{\mathrm{d}(\Gamma - 1)}{\mathrm{d}t} \ll |\Gamma - 1| \tag{A.24}
$$

is valid for all $Q(t)$ or alternatively

$$
\begin{aligned}
&\Gamma^{-1} \frac{\mathrm{d}(\Gamma - 1)}{\dot{Q} V'/V \,\mathrm{d}t} \\
&= \Gamma^{-1} \frac{\mathrm{d}(\Gamma - 1)}{V'/V \,\mathrm{d}Q} \\
&= \frac{\Gamma'}{\Gamma(V'/V)} \ll 1
\end{aligned}
\tag{A.25}
$$

for all $Q(t)$ if one uses the tracker condition (A.5) together with equation (A.24).

For the tracker solution we know that $w_{\tilde{Q}}$ is approximately constant and therefore the time derivatives in the tracker equation (A.23) have to vanish (since $x \equiv \frac{1+w_Q}{1-w_Q}$). The tracker equation then simplifies to

$$\Gamma \approx 1 + \frac{w_B - w_{\tilde{Q}}}{2(1+w_{\tilde{Q}})} \tag{A.26}$$

and we get the following approximation for $w_{\tilde{Q}}$:

$$\begin{aligned}
&\Leftrightarrow (\Gamma - 1)2(1 + w_{\tilde{Q}}) \approx w_B - w_{\tilde{Q}} \\
&\Leftrightarrow 2(\Gamma - 1) + 2(\Gamma - 1)w_{\tilde{Q}} + w_{\tilde{Q}} \approx w_B \\
&\Leftrightarrow w_{\tilde{Q}}\,(2(\Gamma - 1) + 1) \approx w_B - 2(\Gamma - 1) \\
&\Leftrightarrow w_{\tilde{Q}} \approx \frac{w_B - 2(\Gamma - 1)}{1 + (2(\Gamma - 1))}.
\end{aligned} \tag{A.27}$$

If $\Gamma \approx 1$ it follows from equation (A.27) that $w_{\tilde{Q}} \approx w_B$. Since $\frac{d\Gamma}{dw_Q} < 0$ we also find

$$\begin{aligned}
\Gamma > 1 \Leftrightarrow w_{\tilde{Q}} < w_B \\
\Gamma < 1 \Leftrightarrow w_{\tilde{Q}} > w_B
\end{aligned}$$

which gives us a relation between the equation of state of the Q-field and Γ.

Let us now consider the stability of Γ. For this we suppose that w_0 is the equation of state of the tracker solution $\tilde{Q}(t)$ and see what happens with $\Gamma(w_0)$ if it is perturbated by a small amount δ. Since the perturbation δ is very small, we can expand δ and its time-derivatives to the lowest order and consider Γ as constant. The later especially means that $\dot{x}$, $\ddot{x}$, $\dot{w}_0$ and $\ddot{w}_0$ are approximately zero.

To calculate $\delta\Gamma$ we first consider the perturbated terms which are marked with a tilde sign:

$$
\begin{aligned}
\tilde{x} &= \frac{1+w_0+\delta}{1-w_0-\delta} \\
&\approx (1+w_0+\delta)\left(\frac{1}{1-w_0}+\frac{1}{(1-w_0)^2}\delta\right) \\
&= x + \frac{\delta}{1-w_0} + \frac{1+w_0}{(1-w_0)^2}\delta = x + \underbrace{\frac{2}{(1-w_0)^2}}_{a}\,\delta\ , \\
\ln\tilde{x} &= \ln(x - a\,\delta) = \ln x + \ln(1-\frac{a\delta}{x}) \approx \ln x - \frac{a\delta}{x} \\
\dot{\tilde{x}} &\approx \frac{\dot{x}}{x} - \frac{(\dot{a}\delta - a\dot{\delta})x - a\delta\dot{x}}{x^2} = \frac{a\dot{\delta}}{x} \\
\ddot{\tilde{x}} &\approx -\frac{a\,\ddot{\delta}}{x}\ .
\end{aligned}
$$

With the help of these expressions we can calculate the following terms:

$$
\begin{aligned}
\frac{\dot{\tilde{x}}}{6+\dot{\tilde{x}}} &\approx \frac{\frac{a\dot{\delta}}{x}}{6+\frac{a\dot{\delta}}{x}} = \frac{a\dot{\delta}}{a\dot{\delta}+6x} \approx \frac{a\dot{\delta}}{6x}\ , \\
\frac{\ddot{\tilde{x}}}{(6+\dot{\tilde{x}})^2} &\approx \frac{-\frac{a\ddot{\delta}}{x}}{36+12\frac{a\dot{\delta}}{x}} = \frac{-a\ddot{\delta}}{12a\dot{\delta}+36x} \approx -\frac{a\,\ddot{\delta}}{36x}\ .
\end{aligned}
$$

Now we can approximate the perturbated Γ-term by:

$$\begin{aligned}
\Gamma(w_0+\delta) &= 1 + \frac{w_B - w_0 - \delta}{2(1+w_0+\delta)} - \frac{1 + w_B - 2w_0 - 2\delta}{2(1+w_0+\delta)} \frac{\dot{\tilde{x}}}{6+\dot{\tilde{x}}} - \frac{2}{(1+w_0+\delta)} \frac{\ddot{\tilde{x}}}{(6+\dot{\tilde{x}})^2} \\
&\approx 1 + (w_B - w_0 - \delta)\left(\frac{1}{2(1+w_0)} - \frac{1}{2(1+w_0)^2}\,\delta\right) - \frac{1+w_B-2w_0}{2(1+w_0+\delta)} \frac{a\dot{\delta}}{6x} \\
&\quad - \frac{2}{(1+w_0+\delta)} \frac{-a\,\ddot{\delta}}{36x} \\
&\approx 1 + \frac{w_B - w_0}{2(1+w_0)} - \frac{1}{2(1+w_0)}\,\delta - \frac{w_B - w_0}{2(1+w_0)^2}\,\delta \\
&\quad - (1 + w_B - 2w_0)\,\frac{a\dot{\delta}}{2(1+w_0)\,6x} - \frac{2}{(1+w_0)}\,\frac{a\ddot{\delta}}{36x} \\
&\approx 1 + \frac{w_B - w_0}{2(1+w_0)} + \frac{-(1+w_0)-(w_B-w_0)}{2(1+w_0)^2}\,\delta + \frac{-(1+w_B-2w_0)}{2(1+w_0)\,3(1+w_0^2)}\,\dot{\delta} \\
&\quad - \frac{1}{(1+w_0)\,9(1+w_0^2)}\,\ddot{\delta} \\
&\approx 1 + \frac{w_B - w_0}{2(1+w_0)} + \frac{-(1+w_B)}{2(1+w_0)^2}\,\delta + \frac{-(1+w_B-2w_0)}{2(1+w_0)\,3(1+w_0^2)}\,\dot{\delta} \\
&\quad - \frac{1}{(1+w_0)\,9(1+w_0^2)}\,\ddot{\delta}\,.
\end{aligned}$$

This leads to a differential equation for the perturbation δ:

$$\begin{aligned}
&\delta\Gamma(w_0+\delta) - \Gamma(w_0) = 0 \\
&\Leftrightarrow 1 + \frac{w_B - w_0}{2(1+w_0)} - \frac{1+w_B}{2(1+w_0)^2}\,\delta - \frac{1+w_B-2w_0}{2(1+w_0)\,3(1+w_0^2)}\,\dot{\delta} \\
&\quad - \frac{1}{(1+w_0)\,9(1+w_0^2)}\,\ddot{\delta} - \left(1 + \frac{w_B - w_0}{2(1+w_0)}\right) = 0 \\
&\Leftrightarrow -\frac{1+w_B}{2(1+w_0)^2}\,\delta - \frac{1+w_B-2w_0}{2(1+w_0)\,3(1+w_0^2)}\,\dot{\delta} - \frac{1}{(1+w_0)\,9(1+w_0^2)}\,\ddot{\delta} = 0 \\
&\Leftrightarrow \frac{9}{2}(1+w_B)(1-w_0)\,\delta + \frac{3}{2}(1+w_B-2w_0)\,\dot{\delta} + \ddot{\delta} = 0 \\
&\Leftrightarrow \ddot{\delta} + 3\left(\frac{1}{2}(w_B+1) - w_0\right)\,\dot{\delta} + \frac{9}{2}(1+w_B)(1-w_0)\,\delta = 0. \qquad \text{(A.28)}
\end{aligned}$$

The solution of this equation has the form $\delta \propto a^\gamma$ where

$$\begin{aligned}\gamma &= -\frac{3}{2}[\frac{1}{2}(w_B+1)-w_0] \pm \frac{i}{2}\sqrt{18(1+w_B)(1-w_0)-9[\frac{1}{2}(w_B+1)-w_0]^2} \\ &= \alpha \pm \frac{i}{2}\sqrt{\beta}\ . \end{aligned} \tag{A.29}$$

Let us check whether this ansatz solves the differential equation (A.28). Because δ is small we can take γ as time-independent. Notice that the dot now means a derivative with respect to $\ln a$:

$$\begin{aligned}\delta &\sim a(t)^\gamma \\ \dot{\delta} &\sim \gamma\, a^{\gamma-1}\, \dot{a}\, \frac{1}{H} = \gamma\, a^\gamma \\ \ddot{\delta} &\sim \gamma(\gamma-1)\, a^\gamma + \gamma\, a^\gamma\end{aligned}$$

Inserting these expressions yields:

$$\begin{aligned}&\gamma(\gamma-1)+\gamma-2\alpha\gamma+\frac{9}{2}(1+w_B)(1-w_0) \\ &= \alpha^2 \pm i\alpha\sqrt{\beta}-\frac{\beta}{4}-2\alpha^2 \mp 2\frac{i}{2}\alpha\sqrt{\beta}+\frac{9}{2}(1+w_B)(1-w_0) \\ &= -\alpha^2-\frac{1}{4}(18(1+w_B)(1-w_0))+9[\frac{1}{2}(w_B+1)-w_0]^2 \\ &\quad +\frac{9}{2}(1+w_B)(1-w_0) \\ &= -\alpha^2+[\frac{3}{2}(\frac{1}{2}(w_B+1)-w_0)]^2 \\ &= 0\ .\end{aligned}$$

Our ansatz $\delta \propto a^\gamma$ solves the differential equation. The real part of γ (see equation (A.29)) gives the amplitude whereas the imaginary part includes the frequency of the oscillation. Since we prefer the perturbation to vanish, the real part should be negative which is fulfilled for w_0 between -1 and $w_0 = \frac{1}{2}(1+w_B)$. This means that δ vanishes and the solution approaches the tracker solution.

It also means a new restriction for Γ because of equation (A.26). Inserting $\frac{1}{2}(1+w_B)$ for w_Q gives us a lower bound for Γ:

$$\Gamma \approx 1 + \frac{w_B - \frac{1}{2}(1+w_B)}{2(1+\frac{1}{2}(1+w_B))}$$
$$\Gamma \approx 1 + \frac{\frac{w_B}{2} - \frac{1}{2}}{2 + w_B + 1}$$
$$\Gamma \approx 1 - \frac{1-w_B}{6+2w_B} \ . \tag{A.30}$$

Since $\frac{\mathrm{d}\Gamma}{\mathrm{d}w_Q} < 0$ we know that a solution to the equation of motion (see equation (A.4)) is stable if $\Gamma > 1 - (1-w_B)/(6+2w_B)$.
We are now able to give a criterion for tracking behaviour. A potential V has solutions to the equation of motion which are converging to the tracker solution if

$$\boxed{\begin{array}{c} w_Q < w_B \Leftrightarrow \Gamma > 1 \text{ and } \Gamma \approx \text{const.} \\ \text{or} \\ w_B < w_Q < \frac{1}{2}(1+w_B) \Leftrightarrow 1 - \frac{1-w_B}{6+2w_B} < \Gamma < 1 \text{ and } \Gamma \approx \text{const.} \end{array}} \tag{A.31}$$

The advantage of this criterion is that one does not have to solve the equation of motion in order to check the tracking behaviour. It is sufficient to calculate V' and V''.
Instead of $\Gamma > 1$ one can check the two relations $\left(|\frac{V'}{V}|\right) < 0$ and $V' < 0$. The condition $\Gamma < 1$ is equivalent to $\left(|\frac{V'}{V}|\right) > 0$ and $V' < 0$, respectively.

Appendix B

Approximation for the frozen value Q_f

As explained in section 4.2.2, there are two possibilities for the energy density of the scalar field ρ_Q to join the one of the tracker solution $\rho_{\tilde{Q}}$. They are denoted as the undershoot and the overshoot case. We will now give an approximation for the value Q_f at which the energy density ρ_Q freezes for each of the two cases.

B.1 The undershoot case

In the undershoot case one initially has $\rho_{Q_i} < \rho_{\tilde{Q}_i} < \rho_{B_i}$ (recall that ρ_{B_i} denotes the initial value of the background energy density). In this situation, the potential energy of the Q-field is much larger than the kinetic energy and thus $w_{Q_i} \approx -1$. Since the kinetic energy is negligible, the field Q is practically frozen at Q_i until $\rho_{\tilde{Q}}$ (which decreases as the universe evolves) has reached ρ_{Q_i}. Hence, $Q_f \approx Q_i$ in this case.

B.2 The overshoot case

If $\rho_{Q_i} > \rho_{\tilde{Q}_i}$ we are in the overshoot case. Initially, the kinetic energy dominates and one has $w_Q \approx 1$. From this it follows that

$$\rho_Q \simeq \frac{1}{2}\left(\frac{\mathrm{d}Q}{\mathrm{d}t}\right)^2 \sim \rho_Q^0 a^{-6} \,, \tag{B.1}$$

so that, normalizing $a_i = 1$,

$$\frac{\mathrm{d}Q}{\mathrm{d}t} = \left.\frac{\mathrm{d}Q}{\mathrm{d}t}\right|_{t=t_i} a^{-3} \ . \tag{B.2}$$

In order to estimate Q_f we have to solve the differential equation

$$\frac{\mathrm{d}Q}{\mathrm{d}t} = aH\,\frac{\mathrm{d}Q}{\mathrm{d}a} \tag{B.3}$$

which can be rewritten with the help of equation (B.2) as

$$\sqrt{2\rho_{Q_i}} = a^4 H \frac{\mathrm{d}Q}{\mathrm{d}a} \ . \tag{B.4}$$

In order to perform the integration one has to give H in terms of the scale factor. The evolution of H differs according to the dominating energy density component. Therefore, we have to distinguish between the cases $\rho_{B_i} < \rho_{Q_i}$ and $\rho_{Q_i} < \rho_{B_i}$.

B.2.1 $\rho_{Q_i} < \rho_{B_i}$

If the background energy density is initially larger than the one of the scalar field, assuming radiation domination, one has

$$a = \frac{t^{1/2}}{t_i^{1/2}} \tag{B.5}$$

(again, normalizing $a_i = 1$). Consequently, the Hubble parameter is given by

$$H = \frac{1}{2t} = \frac{1}{2a^2 t_i} \ . \tag{B.6}$$

Inserting this into equation (B.4) yields

$$\int_{Q_i}^{Q_f} dQ = \int_1^{a_f} 2t_i\sqrt{2\rho_i}a^{-2}da \tag{B.7}$$

and, since $a_f \gg 1$, one gets

$$Q_f - Q_i \approx 2t_i\sqrt{2\rho_{Q_i}} \ . \tag{B.8}$$

With $H_i = \frac{1}{2t_i} = \sqrt{\kappa\frac{\rho_{Q_i}}{\Omega_{Q_i}}}$ the previous equation can be rewritten as

$$Q_f \approx Q_i + \sqrt{\frac{2\Omega_{Q_i}}{\kappa}} \, . \tag{B.9}$$

B.2.2 $\rho_{Q_i} > \rho_{B_i}$

If the background energy density initially is smaller than the one of the Q-field, the evolution of the scale factor is first dictated by the dominating kinetic energy term, i.e.

$$a = \frac{t^{1/3}}{t_i^{1/3}} \ . \tag{B.10}$$

Therefore, we have

$$H = \frac{1}{3t} = \frac{1}{3a^3 t_i} \tag{B.11}$$

for $\rho_Q > \rho_B$. But as soon as ρ_Q drops below ρ_B we end up in the regime considered in (B.2.1) with $a \sim t^{\frac{1}{2}}$, and therefore we have to be careful with the choice of the limits of the integration. To be more precise: in the range from a_{t_i} to a_{eq} (i.e. the value of the scale factor when $\rho_B = \rho_Q$), we take H according to equation (B.11) and integrating equation (B.4) gives:

$$Q_{eq} = Q_i + 3\sqrt{2\rho_{Q_i}} t_i \ln a_{eq} \tag{B.12}$$

$$= Q_i + \sqrt{\frac{2\Omega_{Q_i}}{\kappa}} \ln a_{eq} \ . \tag{B.13}$$

From the different scaling of ρ_B and ρ_Q with the scale factor, we have $\rho_{B_i} a_{eq}^{-4} = \rho_{Q_i} a_{eq}^{-6}$. Hence, one can rewrite the previous equation as

$$Q_{eq} = Q_i + \frac{1}{2}\sqrt{\frac{2\Omega_{Q_i}}{\kappa}} \ln \frac{\rho_{Q_i}}{\rho_{B_i}} \ . \tag{B.14}$$

The integration from a_{eq} to a_f is in analogy to the case B.2.1, leading to

$$Q_f \approx Q_{eq} + \sqrt{\frac{2\Omega_{Q_i}}{\kappa}} \ . \tag{B.15}$$

Since $\Omega_{Q_i} \approx 1$ in the regime where ρ_{Q_i} dominates, one finally has

$$Q_f \approx Q_i + \sqrt{\frac{2}{\kappa}} \left(1 + \frac{1}{2} \ln \frac{\rho_{Q_i}}{\rho_{B_i}}\right) \ . \tag{B.16}$$

B.3 Summary

Let us summarize the above results: In the undershoot case, we have $Q_i \approx Q_f$. Besides this case, we have two possible values for Q_f depending on whether the initial scalar energy density dominates the one of the background or vice versa. If we initially have $\rho_{Q_i} < \rho_{B_i}$ the frozen value of Q is

$$Q_f \approx Q_i + \sqrt{\frac{2\Omega_{Q_i}}{\kappa}} \tag{B.17}$$

which is a rather small value, since Q_i is typically much smaller than 1 and $\Omega_{Q_i} \approx 10^{-3}$, if one assumes equipartition after inflation. If initially $\rho_{Q_i} > \rho_{B_i}$ instead, the estimation

$$Q_f \approx Q_i + \sqrt{\frac{2}{\kappa}} \left(1 + \frac{1}{2} \ln \frac{\rho_{Q_i}}{\rho_{B_i}}\right) \tag{B.18}$$

holds for the frozen value of Q. Q_f is now much larger than in the previous case according to the ratio of the two energy densities of the scalar field and of the background. In case of the inverse power law potential, the value is typically so large that the scalar energy density is not able to join the tracker solution by the present epoch.

Appendix C

Numerical integration of the equation of motion

Our aim is to integrate the equation of motion of a scalar field Q for a given potential $V(Q)$ numerically in order to understand qualitatively how solutions $Q(t)$ of the equation of motion approach the tracker solution $\tilde{Q}(t)$. In order to get dimensionless units we rescale all occurring quantities in the following way:

$$\tilde{Q} = \frac{Q}{M_P} \tag{C.1}$$

$$\tilde{t} = t \left(\frac{M^{\alpha+4}}{M_P^{\alpha+2}} \right)^{\frac{1}{2}} \tag{C.2}$$

$$\tilde{H} = H \left(\frac{M_P^{\alpha+2}}{M^{\alpha+4}} \right)^{\frac{1}{2}} \tag{C.3}$$

$$\tilde{\rho} = \rho \left(\frac{M_P^{\alpha}}{M^{\alpha+4}} \right) \tag{C.4}$$

$$\frac{\mathrm{d}}{\mathrm{d}\tilde{t}} = \frac{\mathrm{d}}{\mathrm{d}t} \left(\frac{M_P^{\alpha+4}}{M^{\alpha+4}} \right) \tag{C.5}$$

where $M_P \approx 10^{19}$GeV is the Planck scale. With the rescaled quantities, the equation of motion and the Hubble parameter H transform to:

$$\tilde{Q}'' + 3\tilde{H}\tilde{Q}' + \frac{\mathrm{d}\tilde{V}}{\mathrm{d}\tilde{Q}} = 0 \ , \tag{C.6}$$

$$\tilde{H}^2 = \frac{8\pi}{3} \left(\tilde{\rho}_m + \tilde{\rho}_r + \tilde{\rho}_Q \right) \ . \tag{C.7}$$

To improve the numerical stability we rewrite the second order differential equation (C.6) as two differential equations of first order:

$$\Delta(a) \equiv \frac{\mathrm{d}\tilde{Q}}{\mathrm{d}a} \ , \tag{C.8}$$

$$\begin{aligned}\frac{\mathrm{d}\Delta(a)}{\mathrm{d}a} &= -\frac{3}{2a^2}\left(1-\frac{4\pi}{3}a^2\Delta(a)^2\right)\frac{\frac{1}{4\pi}\frac{\mathrm{d}\tilde{V}}{\mathrm{d}\tilde{Q}} - a^{-2}\left(\tilde{\rho}_m^0 + \frac{3}{4}a^{-1}\tilde{\rho}_r^0\right)}{\tilde{V} + a^{-3}\left(\tilde{\rho}_m^0 + a^{-1}\tilde{\rho}_r^0\right)}\Delta(a) \\ &\quad + \frac{4\Delta(a)}{a} - 4\pi a\Delta(a)^3 \ ,\end{aligned} \tag{C.9}$$

$$\tilde{H}^2 = \frac{\frac{8\pi}{3}\left(\tilde{\rho}_m^0 a^{-3} + \tilde{\rho}_r^0 a^{-4} + \tilde{V}\right)}{1 - \frac{4\pi}{3}a^2\Delta\ (a)^2} \ . \tag{C.10}$$

This system of differential equations can be solved by Mathematica or another software for numerical integration.

Bibliography

[1] E. W. Kolb and M. S. Turner, "The early universe,". Redwood City, USA: Addison-Wesley (1990) 547 p. (Frontiers in physics, 69).

[2] N. A. Bahcall, L. M. Lubin, and V. Dorman, "Where is the dark matter?," astro-ph/9506041.

[3] N. A. Bahcall and X. Fan, "A lightweight universe?," astro-ph/9804082.

[4] Boomerang, C. B. Netterfield *et. al.*, "A measurement by boomerang of multiple peaks in the angular power spectrum of the cosmic microwave background," *Astrophys. J.* **571** (2002) 604–614, astro-ph/0104460.

[5] Supernova Cosmology Project, S. Perlmutter *et al.*, "Measurements of omega and lambda from 42 high-redshift supernovae," *Astrophys. J.* **517** (1999) 565–586, astro-ph/9812133.

[6] M. S. Turner and A. G. Riess, "Do SNe Ia provide direct evidence for past deceleration of the universe?," astro-ph/0106051.

[7] N. A. Bahcall, J. P. Ostriker, S. Perlmutter, and P. J. Steinhardt, "The cosmic triangle: Revealing the state of the universe," *Science* **284** (1999) 1481–1488, astro-ph/9906463.

[8] B. P. Schmidt *et al.*, "The high-z supernova search: Measuring cosmic deceleration and global curvature of the universe using type Ia supernovae," *Astrophys. J.* **507** (1998) 46–63, astro-ph/9805200.

[9] A. G. Riess *et al.*, "The farthest known supernova: Support for an accelerating universe and a glimpse of the epoch of deceleration," *Astrophys. J.* **560** (2001) 49–71, astro-ph/0104455.

[10] C. Csaki, N. Kaloper, and J. Terning, "Dimming supernovae without cosmic acceleration," *Phys. Rev. Lett.* **88** (2002) 161302, hep-ph/0111311.

[11] P. Binetruy, "Cosmological constant vs. quintessence," *Int. J. Theor. Phys.* **39** (2000) 1859–1875, hep-ph/0005037.

[12] E. Witten, "The cosmological constant from the viewpoint of string theory," hep-ph/0002297.

[13] B. Ratra and P. J. E. Peebles, "Cosmological consequences of a rolling homogeneous scalar field," *Phys. Rev.* **D37** (1988) 3406.

[14] C. Wetterich, "Cosmology and the fate of dilatation symmetry," *Nucl. Phys.* **B302** (1988) 668.

[15] P. G. Ferreira and M. Joyce, "Cosmology with a primordial scaling field," *Phys. Rev.* **D58** (1998) 023503, astro-ph/9711102.

[16] P. J. Steinhardt, L.-M. Wang, and I. Zlatev, "Cosmological tracking solutions," *Phys. Rev.* **D59** (1999) 123504, astro-ph/9812313.

[17] H. P. Nilles, "Gaugino condensation and supersymmetry breakdown," *Int. J. Mod. Phys.* **A5** (1990) 4199–4224.

[18] I. Zlatev and P. J. Steinhardt, "A tracker solution to the cold dark matter cosmic coincidence problem," *Phys. Lett.* **B459** (1999) 570–574, astro-ph/9906481.

[19] I. Zlatev, L.-M. Wang, and P. J. Steinhardt, "Quintessence, cosmic coincidence, and the cosmological constant," *Phys. Rev. Lett.* **82** (1999) 896–899, astro-ph/9807002.

[20] C. F. Kolda and W. Lahneman, "Exponential quintessence and the end of acceleration," hep-ph/0105300.

[21] J. M. Cline, "Quintessence, cosmological horizons, and self-tuning," *JHEP* **08** (2001) 035, hep-ph/0105251.

[22] Particle Data Group Collaboration, D. E. Groom *et al.*, "Reviews of particle physics," *Eur. Phys. J.* **C15** (2000) 1–878. 2001 off–year partial update for the 2002 edition available on the PDG WWW pages (URL: http://pdg.lbl.gov/).

[23] S. Hellerman, N. Kaloper, and L. Susskind, "String theory and quintessence," *JHEP* **06** (2001) 003, hep-th/0104180.

[24] W. Fischler, A. Kashani-Poor, R. McNees, and S. Paban, "The acceleration of the universe, a challenge for string theory," *JHEP* **07** (2001) 003, hep-th/0104181.